

Authors: Sydney A. Jensen<sup>1</sup>, Jackie R. Webb<sup>1,2</sup>, Gavin L. Simpson<sup>3,4</sup>, Helen M. Baulch<sup>5</sup>, Peter R. Leavitt<sup>1,3</sup>, Kerri Finlay<sup>1,3</sup>

**Affiliations:**

<sup>1</sup> Biology Department, University of Regina, Regina, SK, Canada

<sup>2</sup> Centre for Regional and Rural Futures (CeRRF), Faculty of Science, Engineering and Built Environment, Deakin University, NSW, Australia

<sup>3</sup> Institute of Environmental Change and Society, University of Regina, Regina, Saskatchewan, S4S 0A2, Canada

<sup>4</sup> Present Address: Department of Animal Science, Aarhus University, 8830 Tjele, Denmark

<sup>5</sup> School of Environment and Sustainability and Global Institute for Water Security University of Saskatchewan, Saskatoon, Canada

Corresponding author: Kerri Finlay (kerri.finlay@uregina.ca)

**Contacts:**

SAJ sydney.emmons@uregina.ca; 0000-0001-6671-2172

JRW j.webb@deakin.edu.au; ORCID 0000-0003-1274-363X

GLS gavin@anis.au.dk; ORCID 0000-0002-9084-8413

HMB helen.baulch@usask.ca; ORCID 0000-0001-9018-4998

PRL peter.leavitt@uregina.ca; ORCID 0000-0001-9805-9307

KF kerri.finlay@uregina.ca; ORCID 0000-0001-6835-8832

**Key Points:**

- CO<sub>2</sub>, CH<sub>4</sub>, and N<sub>2</sub>O were correlated with metabolism, conductivity, and primary productivity, respectively.
- Natural ponds were stronger N<sub>2</sub>O sinks than small constructed reservoirs in an agricultural landscape.
- Natural ponds were more frequently GHG sinks, but high CH<sub>4</sub> ebullition resulted in higher mean and max GHG flux than small reservoirs.

**Abstract**

Inland waters are hotspots of greenhouse gas (GHG) emissions, and small water bodies are now well known to be particularly active in the production and consumption of carbon dioxide (CO<sub>2</sub>), methane (CH<sub>4</sub>), and nitrous oxide (N<sub>2</sub>O). High variability in physical, chemical, and environmental parameters affect the production of these GHG, but currently the mechanistic underpinnings are unclear, leading to high uncertainty in scaling up these fluxes. Here, we compare the relative magnitudes and controls of emissions of all three major GHG in twenty pairs of natural wetland ponds and constructed reservoirs in Canada's

largest agricultural region. While gaseous fluxes of  $\text{CO}_2$  and  $\text{CH}_4$  were comparable between the two waterbody types,  $\text{CH}_4$  ebullition was greater in wetland ponds. Carbon dioxide levels were associated primarily with metabolic indicators in both water body types, with primary productivity paramount in agricultural reservoirs, and heterotrophic metabolism a stronger correlate in wetland ponds. Methane emissions were positively driven by eutrophication in the reservoirs, while competitive inhibition by sulfur-reducing bacteria may have limited  $\text{CH}_4$  in both waterbody types. Contrary to expectations,  $\text{N}_2\text{O}$  was undersaturated in both water body types, with wetlands a significantly stronger and more widespread  $\text{N}_2\text{O}$  sink than were reservoirs. These results support the need for natural and constructed water bodies to be considered separately for regional GHG budgets and identification of GHG processing hotspots.

### Plain Language Summary

Small inland water bodies, ponds and reservoirs, are hotspots of greenhouse gas (GHG) emissions, but the underlying controls of the three main GHG are poorly understood. Here we measured emissions and controls of carbon dioxide ( $\text{CO}_2$ ), methane ( $\text{CH}_4$ ), and nitrous oxide ( $\text{N}_2\text{O}$ ) in locally-paired wetland ponds and agricultural reservoirs and found that while GHG emissions were similar in the two waterbody types, underlying mechanisms differed, owing to the differences in shape, depth, and age of individual water bodies. Shallower wetland ponds were typically more fully mixed, exhibited more oxygen at depth, and had higher nutrients and organic carbon concentrations reflecting their ages. Findings suggest that the balance between wetland drainage and reservoir construction may have a pronounced effect regional budgets of GHG fluxes, particularly in the face of forthcoming climate changes.

## 1 Introduction

Small inland waters are well-known hotspots of greenhouse gas (GHG) emissions (Cole et al., 2007; Tranvik et al., 2009) owing to their cumulative abundance in many regions (Downing, 2010) and because they often release carbon dioxide ( $\text{CO}_2$ ) and methane ( $\text{CH}_4$ ) at higher rates than larger inland waters (Downing, 2010). However, GHG concentrations are extremely variable, both spatially and temporally in these small surface waters (Deemer et al., 2016; Downing, 2010; Holgerson & Raymond 2016), with some sites acting as net GHG sinks (Webb et al., 2019a; 2019b). Moreover, relatively few studies quantify fluxes of all three major GHGs ( $\text{CO}_2$ ,  $\text{CH}_4$ , and nitrous oxide,  $\text{N}_2\text{O}$ ) (Huttunen et al., 2002; Liikanen et al., 2006; Ollivier et al., 2019; Whitfield et al., 2011), leading to uncertainties in regional upscaling models and estimates of the importance of small surface waters in estimates of net global warming potential of inland waters (Webb et al., 2019a; 2019b).

Greenhouse gas emissions from wetland ponds have been investigated because of their high global abundance, large sediment carbon pools, and high rates of  $\text{CH}_4$  emissions (Bridgham et al., 2006, Holgerson & Raymond, 2016, Tian

et al., 2016). In the northern Great Plains, there are millions of small prairie wetlands within the ‘Prairie Pothole Region’ that spans 715 500 km<sup>2</sup> across three Canadian provinces (Alberta, Saskatchewan, Manitoba) and five US states (Montana, North Dakota, South Dakota, Minnesota, Iowa) (Bortolotti et al., 2016; Euliss et al., 1999). Such prairie wetlands have been suggested as net carbon sinks suitable for GHG mitigation (Badiou et al., 2011), due to their high productivity and organic carbon sequestration in sediments (Baulch et al. 2021).

Drainage associated with agricultural expansion has eliminated > 40% of wetland ponds in the northern Great Plains (Cortus et al., 2011). Restoration of these wetlands often takes one of two forms; refilling of drained lowland deposits and construction of new agricultural reservoirs. In the first case, in select areas, wetlands have been re-established in the past two decades by building berms and allowing the wetland to refill with precipitation and runoff. Resultant water bodies often exhibit higher rates of CO<sub>2</sub> and CH<sub>4</sub> emission than than undisturbed wetland sites, at least during the first decade after restoration (Bortolotti et al., 2016; Euliss et al., 1999). In contrast, de novo construction of artificial reservoirs is often sited where they will be most useful for agricultural needs and little is known of patterns of net GHG emissions (Webb et al., 2019a; 2019b), particularly in comparison to natural wetland ponds.

Greenhouse gas dynamics can differ between larger natural (e.g., lakes) and human-constructed (e.g., reservoirs) waterbodies, owing to fundamental differences in their morphology, productivity, and watershed characteristics (Hayes et al., 2017). Large reservoirs used to generate hydroelectric power or provide drinking water experience extreme water level fluctuations, leading to changes in hydrostatic pressure and periodic CH<sub>4</sub> ebullition when the water level is reduced (Galy-Lacaux et al., 1999; Joyce & Jewell, 2003; Keller & Stallard, 1994). These reservoirs also typically have higher catchment area to surface area ratios, leading to increased influx of nutrients and organic matter, higher productivity, and elevated respiration and methanogenesis (Davidson et al., 2015; West et al., 2016). In contrast, smaller reservoirs, particularly those in agricultural lands, are used for watering of livestock and to provide relief from both flooding and drought. Small agricultural reservoirs exhibit lower catchment:surface area ratios and their water levels are rarely actively managed. Known locally as ‘dugouts’, small reservoirs often receive nutrient runoff due to their position in the landscape, with surrounding land primarily being used for crop or pastureland. Given these observations, differences in GHG fluxes between natural ponds and small constructed reservoirs are unlikely to follow patterns seen when comparing larger lakes and reservoirs.

Agricultural intensification is increasing the prevalence of small artificial waterbodies across landscapes (Clifford & Heffernan, 2018; Webb et al., 2019b). In contrast to natural wetland ponds, agricultural reservoirs are younger, relatively deeper, and exhibit less emergent vegetation. Worldwide, there are ~440 000 reservoirs  $\leq$  0.1 km<sup>2</sup> covering > 75 000 km<sup>2</sup> of agricultural land (Downing et

al., 2006). Of the limited research to date, studies from Australia (Grinham et al. 2018a; Ollivier et al. 2018, 2019), and India (Panneer Selvam et al., 2014) show that small agricultural reservoirs typically emit  $\text{CO}_2$ ,  $\text{CH}_4$ , and  $\text{N}_2\text{O}$  to the atmosphere. In contrast, work on the northern Great Plains in Canada suggests that although all reservoirs are sources of  $\text{CH}_4$ , more than half of sites ingas  $\text{CO}_2$  (52%) and  $\text{N}_2\text{O}$  (67%) (Webb et al., 2019a; 2019b), suggesting high variation among global agricultural regions.

To accurately upscale GHG emissions from small waterbodies to larger regions, we need a more comprehensive understanding of the underlying mechanisms driving the production of  $\text{CO}_2$ ,  $\text{CH}_4$ , and  $\text{N}_2\text{O}$  in wetland ponds and agricultural reservoirs. In this study, we present a comparative analysis of  $\text{CO}_2$ ,  $\text{CH}_4$ , and  $\text{N}_2\text{O}$  concentration, flux, and regulating factors between natural prairie wetlands and small agricultural reservoirs in the Northern Great Plains, the largest agricultural region in Canada. The aim of this study was to identify whether  $\text{CO}_2$ ,  $\text{CH}_4$ , and  $\text{N}_2\text{O}$  concentrations are of similar magnitude in natural wetlands and agricultural reservoirs, and evaluate which physical, chemical and environmental parameters regulate GHG concentrations in each type of waterbody. To achieve these goals, GHG concentrations were measured in 20 natural wetland ponds paired with 20 co-located agricultural reservoirs in southern Saskatchewan, Canada. By comparing GHG dynamics in paired sites, we are able to isolate the unique effects of basin characteristics (age, morphology, hydrology), as landscape factors such as nutrient loading, climate, and land-use should be comparable. We used generalized additive models (GAMs) to determine the best explanatory covariates of GHG fluxes in each type of waterbody. Our findings show that wetland ponds and agricultural reservoirs exhibit similar concentrations of  $\text{CO}_2$  and  $\text{CH}_4$ , and that natural ponds have significantly lower concentrations of  $\text{N}_2\text{O}$ , but that regulatory mechanisms differed between natural and constructed waterbodies.

## 2 Materials and Methods

Twenty constructed agricultural reservoirs and 20 natural wetland ponds located within the grassland region of Saskatchewan, Canada, were selected for this study (Figure 1A). Each reservoir was paired with a nearby natural wetland to form a single sampling site (mean separation = 280 m, min = 81 m, max = 763 m), with similar landuse around both waterbodies, and no intervening human-made structures (roads, buildings). Each site was sampled once, within a one-month period between 19 June and 15 July 2019.

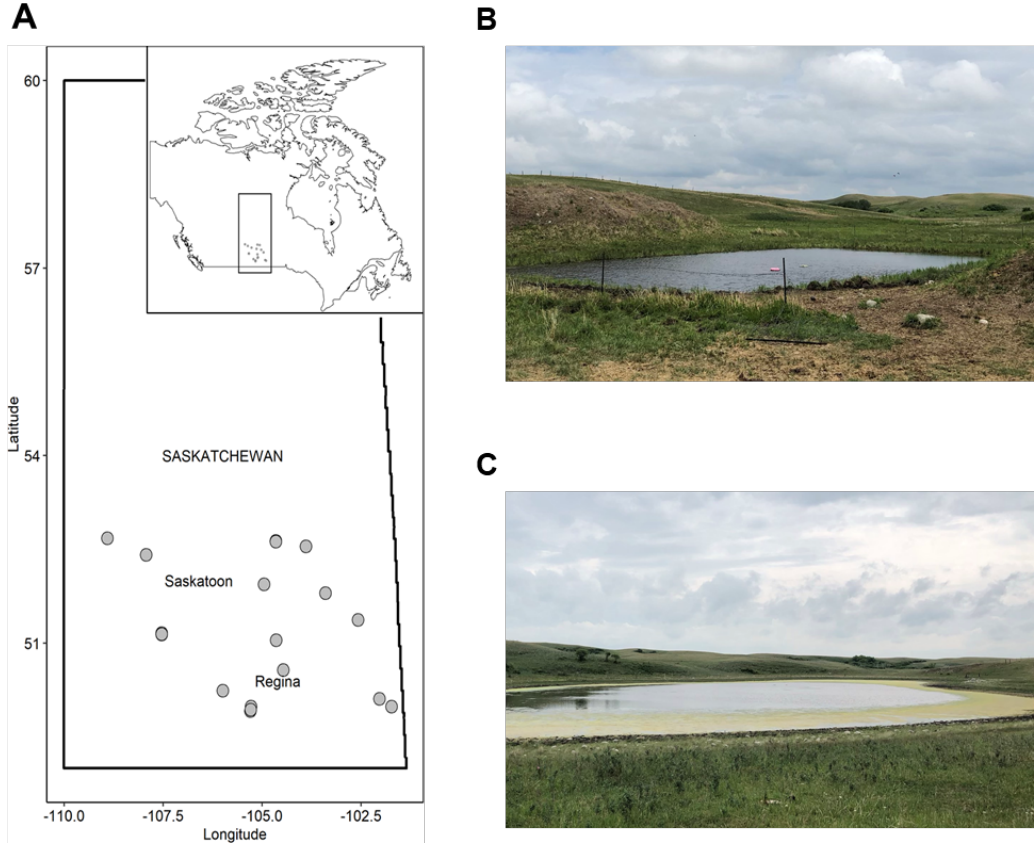


Figure 1. A) Map of locations sampled. Grey circles indicate each of the 20 paired sites sampled during June and July of 2019. Each site is composed of one agricultural reservoir and one natural wetland pond. B) Photo of a typical agricultural reservoir. C) Photo of a natural wetland pond. Photo credit: Sydney Jensen.

## 2.1 Field Collection

When possible, sampling took place from a canoe at the deepest location of each waterbody, although very shallow natural wetlands were sampled by wading, with efforts to minimize sediment perturbation. Samples were collected between 8:45 and 16:30 h. Water parameters including temperature ( $^{\circ}\text{C}$ ), dissolved oxygen (DO,  $\text{mg L}^{-1}$ , % saturation), salinity (g total dissolved solids [TDS]  $\text{L}^{-1}$ ), conductivity ( $\mu\text{S cm}^{-1}$ ), and pH, were measured using a Yellow Springs Instrument (YSI) multi-parameter probe at  $\sim 0.5\text{-m}$  depth intervals from the surface to the bottom. Parameters were estimated at  $0.25\text{-m}$  intervals in very shallow wetlands. Both pH and DO sensors were calibrated prior to measurement at each sampling location. Reservoir depth was taken using a

Norcross Hawkeye handheld depth finder. Average wind speed was measured using a Kestral handheld wind meter at  $\sim 1$  m above the water surface. Water samples were collected using a submersible pump at  $\sim 0.5$  m depth, filtered through 80-  $\mu$ m mesh to remove large zooplankton and particulate matter, and transported to the laboratory within 4 hours of collection.

Concentrations of GHG were estimated using the in-field headspace extraction method (Webb et al., 2019a). Briefly, water was collected from  $\sim 0.5$  m depth using a submersible pump to overfill a 1.2-L glass serum bottle. The bottle was then sealed with a two-way rubber stopper, and a 60-mL sample of atmospheric air was added to the bottle while 60 mL of water was simultaneously removed to maintain constant pressure. The bottle was then shaken vigorously for 2 minutes to equilibrate the air and water. Two replicate gas samples were extracted from the headspace using an air-tight syringe and put into 12-mL pre-evacuated Exetainer vials with double wadded caps. This process was repeated to achieve a total of four gas samples per waterbody, while an atmospheric sample was also collected and placed in similar vial. All gas samples were stored at room temperature until analysis, within 2 months of collection.

Bubble traps with funnel diameter of  $\sim 27$  cm were set up at five sites (5 reservoirs and 5 wetlands) to quantify  $\text{CH}_4$  ebullition rates (DelSontro et al., 2016). In each waterbody, one bubble trap was set in the shallow region ( $\sim 0.5$ -m depth) while a second was set in a central location near where water chemistry was sampled. Shallow-water bubble traps were anchored in place with an iron reinforcing bar driven into sediments, while central traps were attached to an anchored float. All bubble traps were deployed with no headspace to eliminate bubbles at the time of installation. Volume of collected gases was measured monthly for 3 months after installation.

Gas samples were collected to analyze the  $\text{CH}_4$  composition of bubbles formed from the sediments following Baulch et al. (2011). A funnel (30 cm diameter) attached to an air-tight syringe by PVC tubing was submerged under the water surface without trapping air. Bubbles were produced below the funnel by disturbing the sediment with a reinforcing bar. Bubbles were collected until there was enough gas in the funnel for a 12-mL gas sample, after which the sample was transferred to a 12 mL pre-evacuated Exetainer vial as above. The procedure was repeated in duplicate for each site. The dry molar fraction of these gases (in parts per million) were converted to percent composition. Earlier studies of these sites demonstrated that conductivity and sulfate are highly correlated, with inhibition of methanogenesis by sulfate-reducing bacteria when dissolved sulfate levels are high (Webb et al., 2019b). Thus, the relationship between  $\text{CH}_4$  content of bubbles and conductivity was evaluated using a linear regression of %  $\text{CH}_4$  composition and conductivity ( $\log_{10}$ ). The amount of  $\text{CH}_4$  released to the atmosphere was calculated as an areal volumetric daily rate ( $\text{mL m}^{-2} \text{ day}^{-1}$ ) and as a molar ebullition per  $\text{m}^2$  per day ( $\text{mmol m}^{-2} \text{ day}^{-1}$ ). Thus, to estimate ebullitive flux of  $\text{CH}_4$  at all sites, a linear model of conductivity ( $\log_{10}$ ) and  $\text{CH}_4$  ebullition ( $\log_{10}$ ) was run separately for all waterbodies and was used

to extrapolate CH<sub>4</sub> ebullition in unmeasured sites.

## 2.2 Laboratory Analysis

Water samples for chemical analyses were filtered and stored at 4°C within 24 hours of collection. Duplicate water samples for chlorophyll *a* (Chl *a*) were filtered through a Whatman GF/C filter (1.2 µm nominal pore size), wrapped in foil, and frozen (-10°C) until analysis. Filtrate was then passed through a sterile 0.45-µm pore polycarbonate filter, transferred to a 1 L amber glass bottle with no headspace, and stored in the dark at 4°C until analysis at the Institute for Environmental Change and Society, University of Regina. Water chemistry samples were analyzed for soluble reactive phosphorus (SRP), total dissolved phosphorus (TDP), total dissolved nitrogen (TDN), nitrate and nitrite (NO<sub>x</sub>), ammonia (NH<sub>3</sub>), dissolved organic carbon (DOC), and dissolved inorganic carbon (DIC) following Swarbrick et al. (2022). DOC and DIC were analyzed using standard analytic procedures on a Shimadzu model 5000A total carbon analyzer. Dissolved nitrogen species (TDN, NO<sub>x</sub>, NH<sub>3</sub>) and dissolved phosphorus species (TDP, SRP) were measured using standard analytic procedures on a Lachat QuikChem 8500 (Swarbrick et al. 2022). Chlorophyll *a* concentration was measured using standard trichromatic spectrophotometric methods (Finlay et al., 2009; Jeffrey & Humphrey, 1975).

Greenhouse gas samples were analyzed at the Global Institute for Water Security, University of Saskatchewan. Headspace gas samples were analyzed for the dry molar fraction of CO<sub>2</sub>, CH<sub>4</sub>, and N<sub>2</sub>O using a fully calibrated Scion 456 Gas Chromatograph (Bruker Ltd.) with Combipal autosampler (CTC Analytics – PAL System), using argon as the carrier gas. A flame ionization detector was used for methane samples (< 100,000 ppmv). A thermal conductivity detector was used for CO<sub>2</sub> and high level CH<sub>4</sub> concentrations (>100,000 ppmv). N<sub>2</sub>O was measured using a micro-electron capture detector and argon/methane (90/10) as a makeup gas (injector temperature 60°C, column temperature 60°C, detector temperature 350°C). All gases were calibrated using mixed gas standards (Praxair) with the addition of a single gas N<sub>2</sub>O standard (0.1ppmv; Scotty).

## 2.3 Numerical Analyses

The dry molar fraction of CO<sub>2</sub>, CH<sub>4</sub>, and N<sub>2</sub>O were corrected for dilution with on-site atmospheric air and converted to concentrations according to the gas-specific solubility coefficients, atmospheric pressure, and salinity (Weiss, 1974; Weiss & Price, 1980; Yamamoto et al., 1976). Four replicate gas concentrations were averaged to obtain estimates of CO<sub>2</sub>, CH<sub>4</sub>, and N<sub>2</sub>O at each site. Dissolved concentrations of each gas were used to estimate the diffusive flux ( $f_C$ ) of CO<sub>2</sub>, CH<sub>4</sub>, and N<sub>2</sub>O using the gas transfer velocity ( $k_c$ ), gas concentration of the water ( $C_{\text{water}}$ ), and the ambient air concentration ( $C_{\text{air}}$ ) following equation (Equation 1):

$$f_C = k_c (C_{\text{water}} - C_{\text{air}}). \quad (1)$$

Mean air concentrations were 413.09  $\mu\text{atm}$  for  $\text{CO}_2$ , 1.868  $\mu\text{atm}$  for  $\text{CH}_4$ , and 0.333  $\mu\text{atm}$  for  $\text{N}_2\text{O}$ . Diffusive flux was calculated using the gas transfer velocity for small, low wind lakes (Cole & Caraco, 1998), and using an average measured mean wind speed of 2.32  $\text{m s}^{-1}$  across all sites.

The squared Brunt-Väisälä buoyancy frequency ( $\text{s}^{-2}$ ) was calculated as a measure of maximum stratification strength within the water column. This approach uses the steepest in situ density gradient observed for water temperature profiles taken at 0.5 m intervals (0.25 m in shallow waterbodies) and was calculated using the *rLakeAnalyzer* package (Read et al., 2012) in R (version 4.0.5; R Core Team, 2021) following Webb et al. (2019b).

To determine if differences in GHG concentrations were significantly different between natural and constructed waterbodies, we used a one-sample Wilcoxon signed rank test with  $\alpha = 0.05$ . The Wilcoxon test was chosen over a one-sample t-test because pond data were not normally distributed.

Carbon dioxide equivalent ( $\text{CO}_2\text{-eq}$ ) flux was calculated using the sustained flux global warming potential model if fluxes were above zero, and with the cooling potential model if fluxes were negative (Neubauer & Megonigal, 2015). Diffusive flux values of  $\text{CH}_4$ , and  $\text{N}_2\text{O}$ , as well as the ebullitive flux of  $\text{CH}_4$ , were converted to the same units before multiplication by the appropriate warming or cooling potential, and summation across gases to give the total  $\text{CO}_2\text{-eq}$  flux for each site.

Generalized additive models (GAMs, Wood, 2017; Wood et al., 2016) were used to determine the relationships between physical, chemical, and environmental factors and concentrations of  $\text{CO}_2$ ,  $\text{CH}_4$ , and  $\text{N}_2\text{O}$  in natural ponds and agricultural reservoirs. Covariates included as predictors in the models were chosen based on the basis of prior knowledge of biotic and abiotic factors known to influence production or consumption of each GHG (Webb et al., 2019a, 2019b). Variables included as smoothed terms included nutrients (DOC, DIN, and SRP), DOC to nutrient ratios (DOC:  $\text{NO}_x$ , DOC:SRP), productivity (Chl a, and DO), and stratification strength (buoyancy frequency). Conductivity was added into the  $\text{CH}_4$  model as a proxy for sulfate concentrations, the main regional anion. We selected GAMs for this analysis because of their ability to model linear, nonlinear, and nonmonotonic relationships between response and predictor variables (Monteith et al., 2014; Orr et al., 2015; Swarbrick et al. 2019; Webb et al., 2019a; 2019b). All modelling was done using the *mgcv* software package (Wood, 2011; Wood et al., 2016) within the R computational environment (version 4.0.5; R Core Team, 2021).

Waterbody type was included as a parametric fixed effect in the models, and a factor-smooth interaction was used for each smooth term to allow the smooth effects of each covariate in the model to vary between ponds and reservoirs. The gas concentration ( $\text{CO}_2$  and  $\text{CH}_4$ ) was assumed to be conditionally distributed gamma (loglink function) resulting in a GAM that is suitable for positive continuous responses.  $\text{N}_2\text{O}$  had no link function used as it was normally



distributed without transformation. Basis size, dispersion of residuals, homogeneity of variance, and the relationship between the observed and predicted response were assessed in each model to ensure assumptions were not violated. Residual marginal likelihood (REML) was used for selection of smoothness parameters (Wood, 2011). To help with model selection, the double penalty approach of Marra & Wood (2011) was used. An additional penalty is applied to the perfectly smooth parts of the basis (the functions in the penalty null space) of each smooth function in the model, which allows entire smooths to be effectively penalised out of the model, while accounting for the selection procedure in the statistical tests applied to model terms. Parameters predicting  $\text{CO}_2$ ,  $\text{CH}_4$ , and  $\text{N}_2\text{O}$  concentrations were considered significant at 95% confidence level ( $\alpha = 0.05$ ) for each waterbody.

### 3 Results

#### 3.1 Water Quality

Physical and chemical conditions varied between agricultural reservoirs and natural wetland ponds (Table 1). In general, wetland ponds were shallower (0.6 m) than reservoirs (2.7 m) and had higher concentrations of DOC, DIC, TN, and TP, but lower DO concentration. In contrast, reservoirs had significantly greater relative depth (ratio of max. depth to average diameter, 8.3 %) compared to wetlands (1.1 %). Concentrations of SRP, NOx, and ammonia were comparable between wetlands and reservoirs, as were surface water temperatures and Chl *a* concentrations, although reservoirs had a much larger range of Chl *a* concentration than did natural wetlands (Table 1). Conductivity was not statistically different between the waterbody types, although wetlands' mean was skewed by two high values (14899 and 18975  $\mu\text{S cm}^{-1}$ ).

#### 3.2 Greenhouse Gas Concentrations

Concentrations of  $\text{CO}_2$  and  $\text{CH}_4$  were comparable between natural wetland ponds and agricultural reservoirs, while  $\text{N}_2\text{O}$  was significantly lower in wetland environments (Table 1). Eight reservoirs and 14 wetlands were undersaturated in  $\text{CO}_2$  whereas all wetlands and 18 reservoirs were supersaturated with  $\text{CH}_4$ . Most reservoirs and wetlands were undersaturated in  $\text{N}_2\text{O}$ , with only one wetland and four reservoirs being supersaturated.

Ebullition rates from deep sediments were comparable between wetlands and reservoirs, with average gas emission rates of 182  $\text{mL m}^{-2} \text{ day}^{-1}$  (SD = 138) and 220  $\text{mL m}^{-2} \text{ day}^{-1}$  (SD = 176), respectively (Wilcoxon rank test, p-value = 0.14). Changes in water levels caused the exposure of bubble traps to air between sampling intervals in the nearshore shallow regions hindering the collection of ebullition rates at these locations. Based on ebullition data collected from agricultural reservoirs in the 2018 seasonal study (Jensen 2021), ebullition rates were comparable between the deep and shallow regions, therefore only deep ebullition rates were used here. Composition of fresh bubbles from sediments

differed slightly in CH<sub>4</sub> content among waterbody types, with wetland bubbles being  $15.6 \pm 26.6$  % CH<sub>4</sub> (mean  $\pm$  SD) and reservoirs being  $4.9 \pm 9.7$ % CH<sub>4</sub>. Bubble composition was significantly negatively correlated with conductivity (as a proxy for sulfate concentration) in both wetland ponds and reservoirs, suggesting inhibition of methanogenesis at higher sulfate levels in all sites (Fig S3). The regression had a significantly higher intercept in wetland ponds, indicating that more CH<sub>4</sub> is produced in bubbles in wetland ponds, compared to reservoirs (Fig S3, Analysis of Covariance [ANCOVA] p-value = 0.022).

Predicted CH<sub>4</sub> ebullition (Figure 2) was calculated using the linear regression (Supplementary Figure S4) of conductivity (log<sub>10</sub>) and CH<sub>4</sub> ebullition (log<sub>10</sub>) for reservoirs (adj. R<sup>2</sup> = 0.60) and for wetlands (adj. R<sup>2</sup> = 0.77). The mean predicted CH<sub>4</sub> ebullitive flux for reservoirs was 0.51 mmol m<sup>-2</sup> day<sup>-1</sup> (SD = 0.93) and 8.84 mmol m<sup>-2</sup> day<sup>-1</sup> (SD = 24.2) in wetlands. While the mean predicted ebullition rate is higher in natural wetland ponds, this difference is not statistically significant due to the variability observed within the wetlands (Wilcoxon rank test, p-value = 0.37).

Table 1. Physical and chemical parameters for pairs of 20 agricultural reservoirs and 20 natural wetland ponds during 2019. Values presented as mean  $\pm$  standard deviation. Significance represents results from a Wilcoxon rank tests at \* p<0.1; \*\* p<0.05; \*\*\* p<0.01. DO = dissolved oxygen. DIC = dissolved inorganic carbon. DOC = dissolved organic carbon. TDP = total dissolved phosphorus. SRP = soluble reactive phosphorus. TDP = total dissolved nitrogen. NO<sub>x</sub> = nitrate and nitrite. NH<sub>3</sub> = ammonia. Chl a = chlorophyll a. CO<sub>2</sub> = carbon dioxide. CH<sub>4</sub> = methane. N<sub>2</sub>O = nitrous oxide, max = maximum.

Parameter	Units	Mean (SD)	
		Reservoirs	Wetlands
Water Temperature	°C	20.4 (2.8)	20.6 (3.1)
Max Depth	meters	2.7 (1.0) ***	0.6 (0.5)
Relative Depth	%	8.3 (4.2) ***	1.1 (1.5)
Buoyancy Frequency	s <sup>-2</sup>	0.011 (0.01) ***	0.005 (0.009)
pH	Unitless	8.8 (0.7)	9.1 (0.6)
Surface DO	% Sat.	95.7 (32.8)	109.5 (38.7)
Deep DO	% Sat.	24.5 (39.2)	84.8 (48.6) ***
Conductivity	µS cm <sup>-1</sup>	1495.4 (1460.2)	3336.9 (5078.0)
DIC	mg C L <sup>-1</sup>	51.5 (25.8)	60.5 (34.6)
DOC	mg C L <sup>-1</sup>	28.9 (12.9)	53.8 (29.2) ***
Alkalinity	mg L <sup>-1</sup>	226.1 (108.9)	295.7 (155.5)
TDP	µg P L <sup>-1</sup>	248.5 (385.3)	449.5 (600.3) **
SRP	µg P L <sup>-1</sup>	204.8 (344.6)	341.0 (568.4)
TDN	µg N L <sup>-1</sup>	2048.8 (1107.4)	3515.5 (2087.6) ***
NO <sub>x</sub>	µg N L <sup>-1</sup>	272.3 (367.6)	113.0 (129.1)
NH <sub>3</sub>	µg N L <sup>-1</sup>	71.1 (103.3)	100.8 (91.4)
Chl a	µg L <sup>-1</sup>	43.7 (85.8)	13.2 (16.7)
CO <sub>2</sub>	µM	30.1 (44.3)	37.6 (90.4)

CH <sub>4</sub>	μM	1.3 (1.7)	1.4 (1.7)
N <sub>2</sub> O	nM	8.3 (2.2) ***	6.3 (1.6)

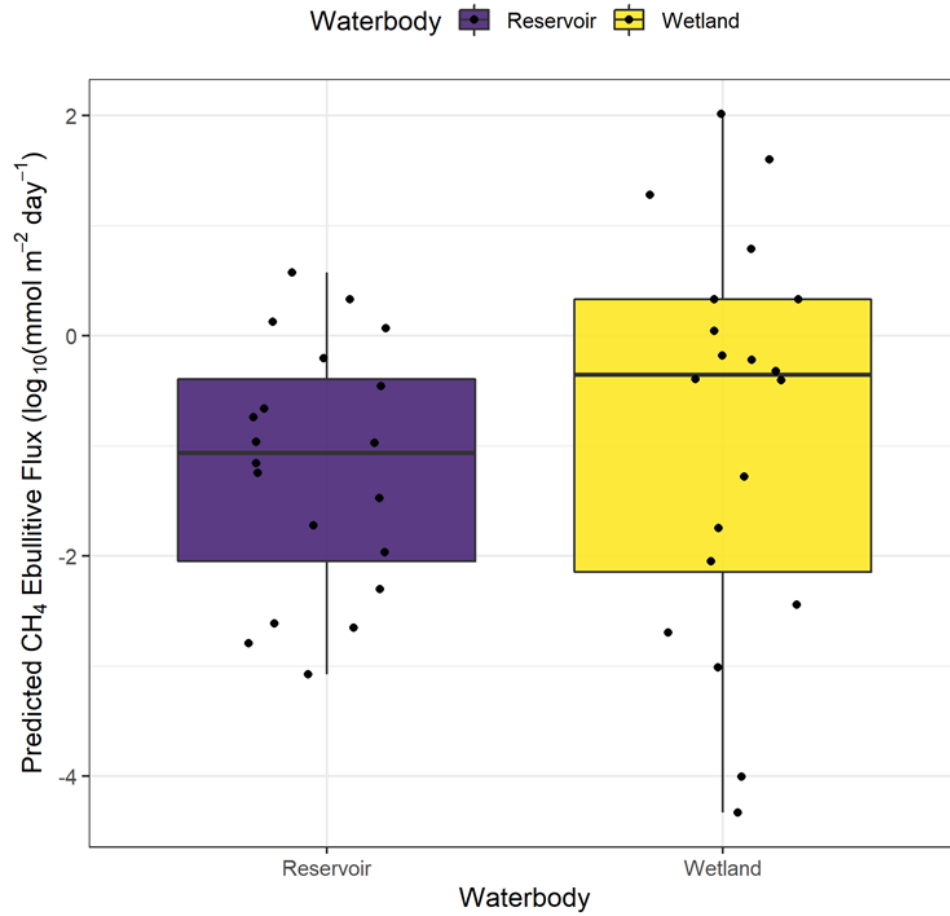


Figure 2. Predicted CH<sub>4</sub> (log<sub>10</sub>) ebullitive flux rates from agricultural reservoirs and natural wetland ponds. Predicted from relationship between CH<sub>4</sub> ebullition and conductivity (see Supplementary Figure S3). Results from a Wilcoxon Rank Test indicate the ebullitive flux of CH<sub>4</sub> does not differ between reservoirs and wetlands at  $\alpha = 0.05$ ,  $n = 20$  pairs of waterbodies. Boxplot shows the median (center line), 75<sup>th</sup> and 25<sup>th</sup> percentiles (upper and lower hinges, respectively; difference between 25<sup>th</sup> and 75<sup>th</sup> percentile is the interquartile range), 1.5x the interquartile range above the 75<sup>th</sup> percentile (upper whisker) and below the 25<sup>th</sup> percentile (lower whisker). Black points are raw data.

### 3.3 Controls of Greenhouse Gas Concentration

GAMs including only pH best estimated  $\text{CO}_2$  concentrations in both reservoirs and wetlands, explaining 83% of deviance and exhibiting a strong negative relationship between pH and  $\text{CO}_2$  concentrations in both waterbodies (Figure 3). When pH was not included in the GAMs,  $\text{CO}_2$  concentrations were best estimated by a combination of physical and chemical parameters in both agricultural reservoirs and natural wetland ponds explaining 87.7 % of deviance. However, in this case, predictors of  $\text{CO}_2$  concentrations differed between waterbody types with significant predictors ( $p < 0.05$ ) in reservoirs including DO saturation (negative), chlorophyll *a* (positive), and ratios of  $\text{DOC}:\text{NO}_x$  (negative), whereas in wetlands parameters included alkalinity (positive), buoyancy frequency (positive) and  $\text{DOC}:\text{NO}_x$  (unimodal).

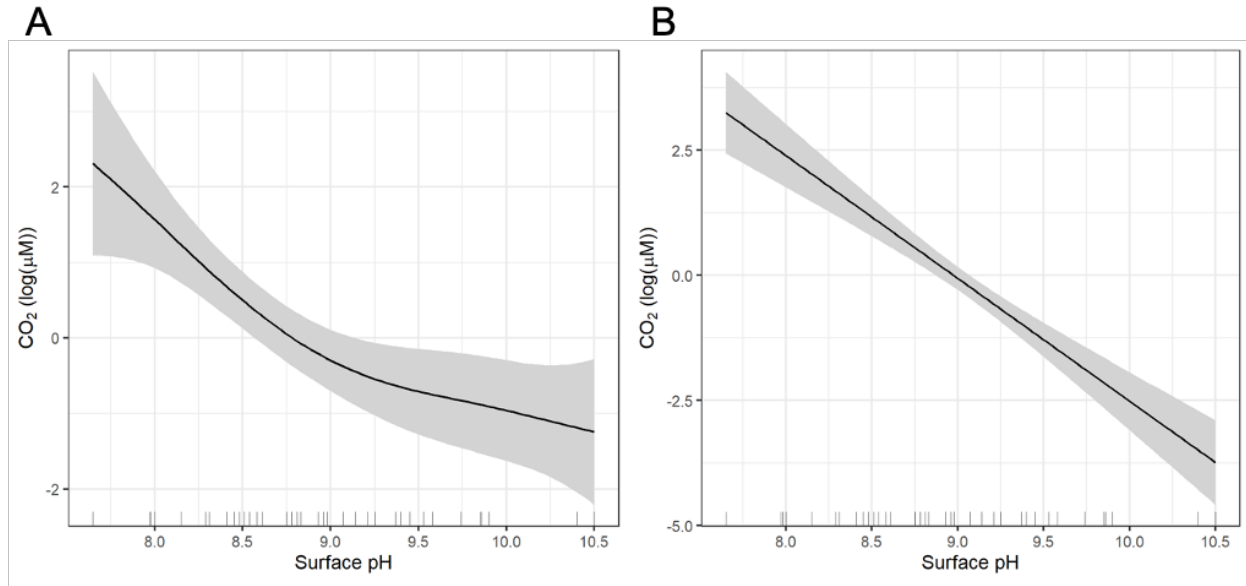


Figure 3. Partial effects plots from the generalized additive model assessing the relationship between pH and  $\text{CO}_2$  concentration in (a) reservoirs and (b) wetlands. Deviance explained = 83%. Grey shaded region represents the 95% Bayesian credible interval. Rugs on x-axis represent measured data points.

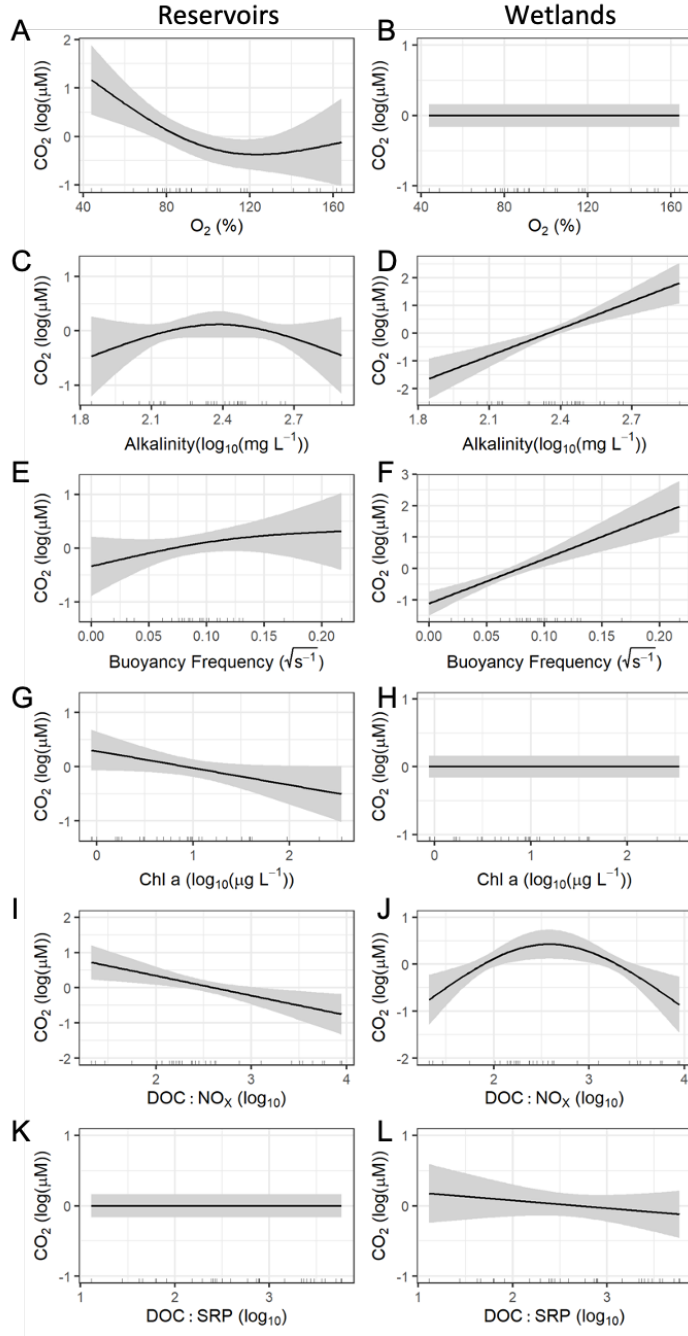


Figure 4. Partial effects plots from the generalized additive model relating  $\text{CO}_2$  in reservoirs (left) and wetlands (right) to water column conditions. Overall deviance explained = 87.7%. Grey shaded region represents the 95% Bayesian

credible interval. Rugs along the x-axis represent the measured data points. Covariates included dissolved oxygen (A, B), alkalinity C, D), buoyancy frequency (E, F), chlorophyll *a* (chl *a*; G, H), ratios of dissolved organic carbon to nitrate (DOC:NO<sub>3</sub><sup>-</sup>; I, J), and ratios DOC to soluble reactive phosphorus ratio (DOC:SRP; K, L).

Methane concentrations were best estimated in a GAM by a combination of physical, chemical, and biological parameters in both waterbodies with 86.2% deviance explained (Figure 5). Significant predictors ( $p < 0.05$ ) of CH<sub>4</sub> in reservoirs included surface DO saturation (negative), chlorophyll *a* (positive), conductivity (unimodal), buoyancy frequency (negative), and DOC:NO<sub>x</sub> (positive). In wetlands, the significant predictors of CH<sub>4</sub> were conductivity (negative) and buoyancy frequency (positive).

Nitrous oxide concentrations were best estimated in a GAM by a combination of biotic and abiotic parameters with 95.8 % deviance explained (Figure 6). The significant predictors between reservoirs and wetlands were similar, with surface DO saturation, NO<sub>x</sub> concentration, and chlorophyll *a* being significant, although the nature of the relationships differed between waterbodies. Wetlands exhibited decreasing N<sub>2</sub>O concentrations as DO increased, while reservoirs exhibited a positive relationship with DO. Reservoirs showed increasing N<sub>2</sub>O concentrations with increasing NO<sub>x</sub> concentrations, whereas wetlands exhibited decreasing gas concentrations. Both waterbodies had significant relationships between N<sub>2</sub>O concentrations and Chl *a* concentrations, with a negative relationship in reservoirs, and a unimodal relationship in wetlands with maximum N<sub>2</sub>O at ~18 µg N L<sup>-1</sup>. Additionally, DOC concentration was weakly positive in reservoirs, whereas wetlands exhibited a decreasing trend in N<sub>2</sub>O as DOC increased.

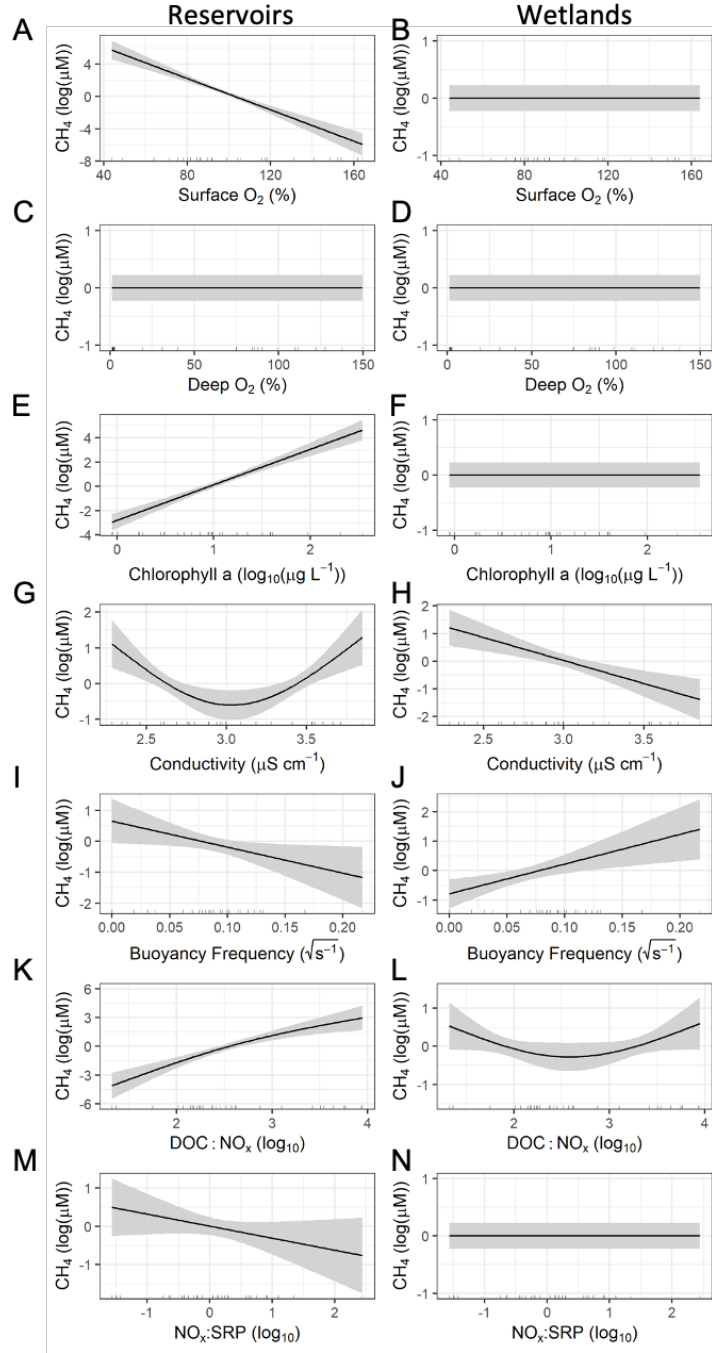


Figure 5. Partial effects plots from the generalized additive model relating dissolved  $\text{CH}_4$  concentration to environmental conditions in reservoirs (left) and

wetlands (right). Deviance explained = 86.2%. Grey shaded region represents the 95% Bayesian credible interval. Rugs along the x-axis represent the measured data points. Covariates include surface dissolved oxygen ( $O_2$ ) (A, B), deep  $O_2$  (C, D), chlorophyll a (chl a; E, F), conductivity (G, H), buoyancy frequency (I, J), ratios of dissolved organic carbon (DOC) to  $NO_x$  (DOC: $NO_x$ ; K, L) and ratios of nitrate/nitrite to soluble reactive phosphorus ( $NO_x$ :SRP; M, N).



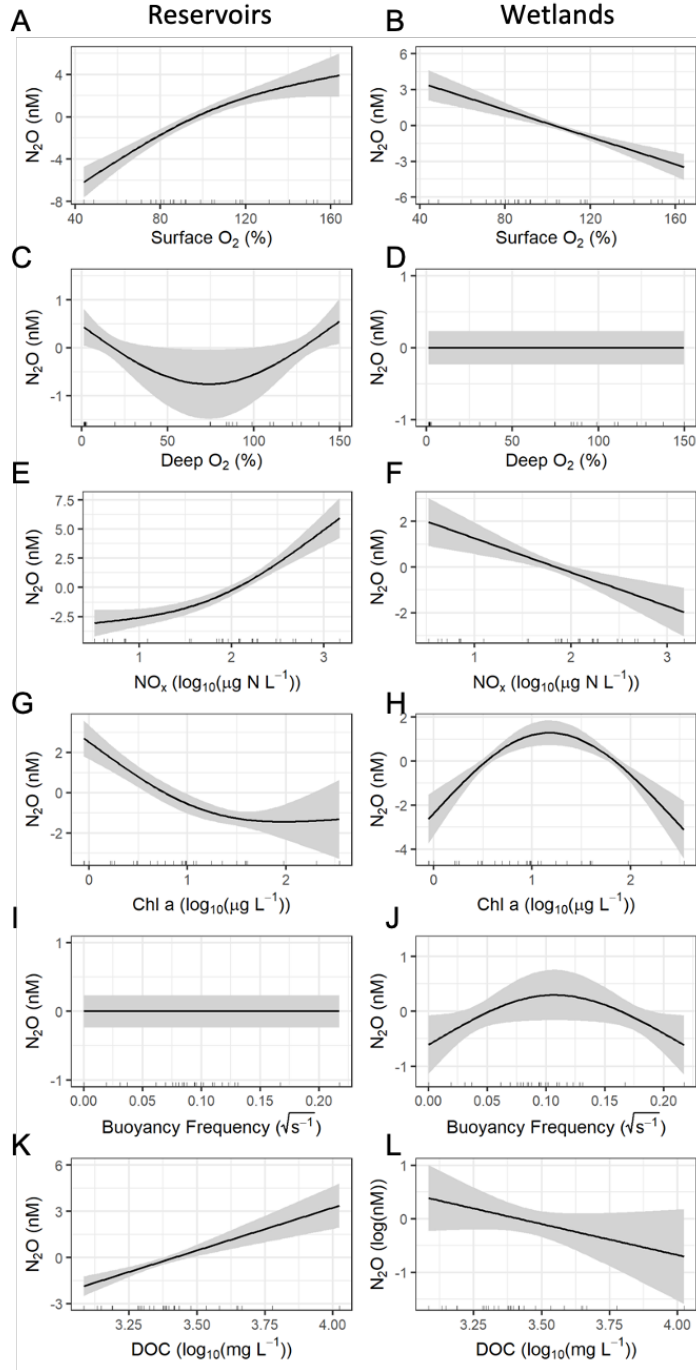


Figure 6. Partial effects plots from the generalized additive model relating

nitrous oxide ( $\text{N}_2\text{O}$ ) concentrations to environmental conditions in reservoirs (left) and wetlands (right). Deviance explained = 95.8%. Grey shaded region represents the 95% Bayesian credible interval. Rugs along the x-axis represent the measured data points. Covariates include surface dissolved oxygen ( $\text{O}_2$ ; A, B), deep  $\text{O}_2$  content (C, D), nitrate/nitrite ( $\text{NO}_x$ ; E, F), chlorophyll a (chl a; G, H), buoyancy frequency (I, J), and dissolved organic carbon (DOC; K, L).

### 3.4 Greenhouse Gas Fluxes, and Regional Scaling

Mean  $\text{CO}_2$  diffusive flux calculated over all waterbodies was  $43.9 \text{ mmol m}^{-2} \text{ day}^{-1}$  ( $\text{SD} = 150.2$ ), while  $\text{CO}_2$  flux values were slightly less in reservoirs ( $36.5 \pm 10.7 \text{ mmol m}^{-2} \text{ day}^{-1}$ ) than in wetlands ( $51.2 \pm 187.0 \text{ mmol m}^{-2} \text{ day}^{-1}$ ; Figure 7A). Mean  $\text{CH}_4$  diffusive flux over all sites was  $3.3 \pm 4.0 \text{ mmol m}^{-2} \text{ day}^{-1}$ , with similar values in reservoirs ( $3.1 \pm 4.0 \text{ mmol m}^{-2} \text{ day}^{-1}$ ) and wetlands ( $3.4 \pm 4.1 \text{ mmol m}^{-2} \text{ day}^{-1}$ ; Figure 7C). Release of  $\text{CH}_4$  through ebullitive flux was comparable at 5 reservoirs ( $1.4 \pm 2.2 \text{ mmol m}^{-2} \text{ day}^{-1}$ ) and agricultural reservoirs ( $0.7 \pm 1.4 \text{ mmol m}^{-2} \text{ day}^{-1}$ ). Ebullitive flux of  $\text{CH}_4$  predicted from conductivity concentrations of all sites was  $0.5 \pm 1.0 \text{ mmol m}^{-2} \text{ day}^{-1}$  in reservoirs and  $8.8 \pm 24.2 \text{ mmol m}^{-2} \text{ day}^{-1}$  in wetland ponds (Figure 7C). Finally, mean diffusive flux of  $\text{N}_2\text{O}$  flux in all waterbodies was  $-3.4 \pm 4.8 \text{ } \mu\text{mol m}^{-2} \text{ d}^{-1}$ , while that of wetland ponds was  $-5.6 \pm 3.3 \text{ } \mu\text{mol m}^{-2} \text{ d}^{-1}$  and reservoirs was  $-1.1 \pm 5.0 \text{ } \mu\text{mol m}^{-2} \text{ d}^{-1}$ , with 20% of the sites being net sources of  $\text{N}_2\text{O}$  to the atmosphere (Figure 7B).

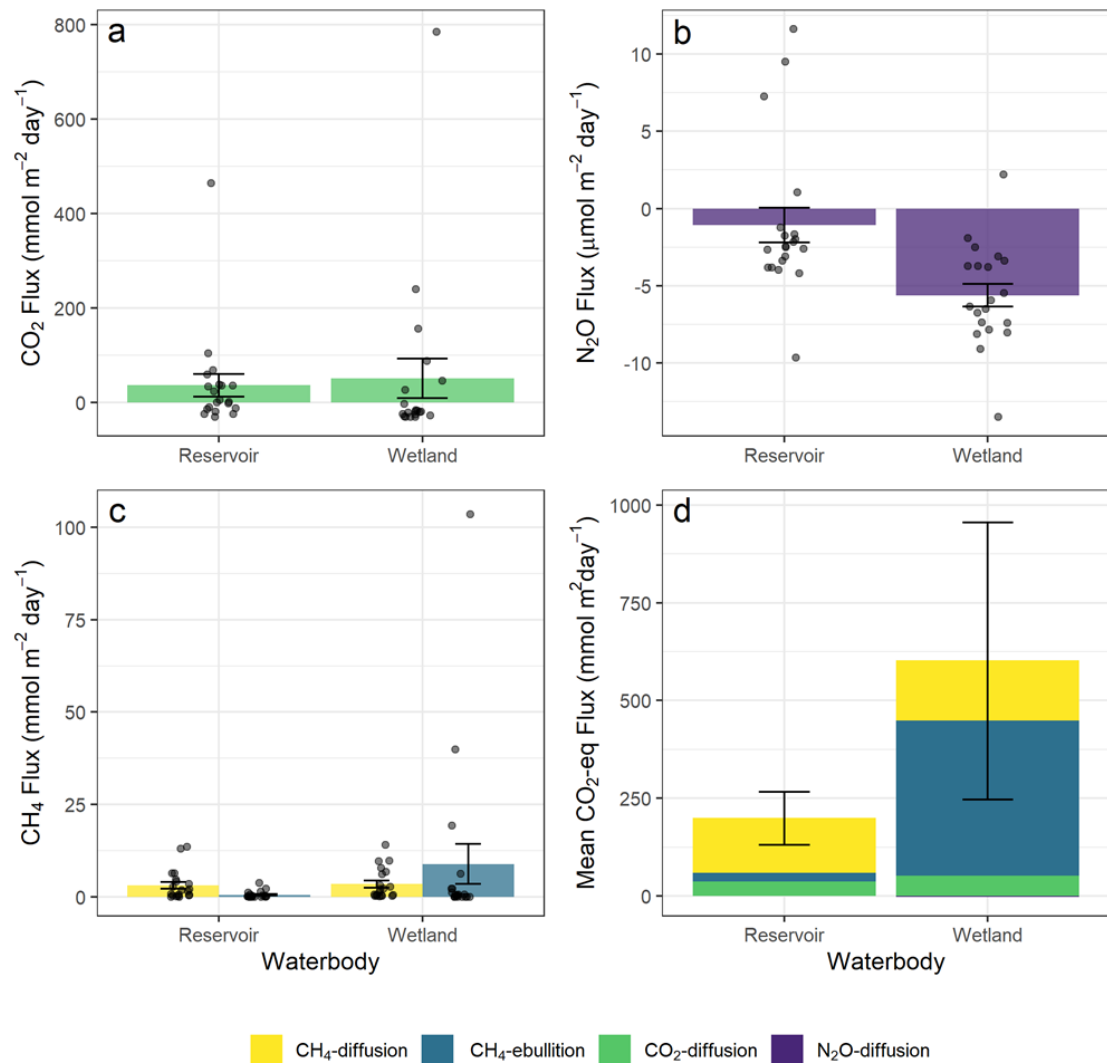


Figure 7. Diffusive fluxes of A) CO<sub>2</sub>, B) N<sub>2</sub>O, and C) CH<sub>4</sub> flux (all mmol m<sup>2</sup> day<sup>-1</sup>), as well as ebullitive flux of CH<sub>4</sub> predicted from log-log relationship with conductivity (see Supplementary Figure S3). D) CO<sub>2</sub>-equivalent flux aggregated by each gas. All panels presented as mean  $\pm$  standard deviation. Panel D) error bars are calculated on the mean total CO<sub>2</sub>-eq flux.

#### 4 Discussion

Loss of natural wetlands, combined with increased construction of small farm reservoirs, has the potential to alter landscape patterns of GHG flux from continental grasslands. Here we found that while fluxes of CO<sub>2</sub> and CH<sub>4</sub> did not

differ substantially between constructed reservoirs and wetland ponds, potential regulatory mechanisms varied among waterbody types (Figs 4-6). The variation likely reflected differences in basin morphology and stratification (Kalff & Downing, 2016, Qin et al., 2020), as well as DOC quality or quantity (Waiser and Robarts 2004). Furthermore, natural wetlands were more substantial sinks of atmospheric  $\text{N}_2\text{O}$  than artificial waters, with marked  $\text{N}_2\text{O}$  undersaturation in most waterbodies (Webb et al. 2019). Differences in regulatory mechanisms suggest that each waterbody needs to be considered separately in inland water emission models and development of future GHG management strategies for farms.

#### 4.1 Physical and Chemical Comparison of Wetland Ponds and Agricultural Reservoirs

While agricultural reservoirs and natural ponds had comparable concentrations of most measured water chemistry variables, waterbody morphometry and thermal stratification were significantly different between surface water types (Table 1), with potential cascading effects on concentrations of DOC, TDN, and TDP. Elevated DOC, TDN, and TDP levels may be attributable to older age, shallower depth, and less stable water column in the wetland ponds (Kalff & Downing, 2016). Similarly, a review of 573 global lakes showed that TN and TP concentrations decrease with increasing water depth, in part reflecting differences in mixing depth and the area of sediment in contact with the overlying water (Qin et al., 2020). Agricultural reservoirs were often thermally stratified during the monitoring period (data not shown), while natural wetlands were not due to their shallow depth (mean = 0.6 m), larger surface area (mean = 16 425  $\text{m}^2$ ), and greater exposure to wind due to absence of lateral excavation spoil piles (Kalff & Downing, 2016). We observed a strong correlation between wetland depth and SRP (Spearman  $\rho$  = -0.61; Supplementary Figure S2); however, only weak to moderately-strong relationships ( $\rho$  = -0.04 and -0.31) between SRP, TDN and depth in reservoirs, and DOC was only moderately correlated to depth or stratification strength (as buoyancy frequency) in both waterbodies (Supplementary Figure S1 and S2). These patterns suggest that differences in morphology arising from mode of origin (lowland flooding, construction) had substantial effects on chemical characteristics that impacted GHG production and loss from the different waterbody types.

#### 4.2 Regulation of Carbon Dioxide Concentration

Carbon dioxide concentrations were comparable in reservoirs and natural ponds, with gas levels correlated strongly with changes in pH, a pattern characteristic of hardwater lakes with pronounced carbonate buffering (Duarte et al., 2008; Finlay et al., 2015; Stumm & Morgan, 1970; Wiik et al., 2018; Webb et al., 2019b). When effects of pH were removed from the models,  $\text{CO}_2$  concentrations were found to be strongly influenced by metabolic processes in both waterbody types, with wetlands demonstrating evidence of primarily benthic respiration,

while reservoirs demonstrated a stronger influence of epilimnetic primary production.

In natural ponds, there was a significant unimodal relationship between  $\text{CO}_2$  and  $\text{DOC:NO}_x$  concentrations, but the lack of relationship between  $\text{CO}_2$  and chlorophyll *a* suggests that heterotrophic metabolism was controlling  $\text{CO}_2$  concentrations (Bogard et al., 2017, Webb et al 2019b) by remineralizing organic matter (Maher et al., 2019), likely in the sediments. While we observed a general relationship between buoyancy frequency and  $\text{CO}_2$  concentrations in natural ponds, only seven of the 20 sites exhibited thermal stratification, suggesting that stratification was not a broadly important mechanism regulating gas flux. We had expected that wetland ponds would experience less profound or persistent thermal stratification than the deeper agricultural reservoirs, particularly given the larger surface areas and shallower depths characteristic of wetland ponds (Kalfs & Downing, 2016). Interestingly, we did not observe any metabolic relationship between changes in  $\text{O}_2$  and  $\text{CO}_2$  concentrations in wetland ponds, in contrast to patterns seen in other shallow small ponds (Holgerson, 2015; Bortolotti et al., 2016) and our small agricultural reservoirs (Fig. 4). We suggest that uncoupling of  $\text{CO}_2$  and DO may reflect strong carbonate buffering, such as seen in other DIC-rich systems (Stets et al., 2017; Vachon et al., 2020), supported by the significant positive relationship between  $\text{CO}_2$  concentrations and DIC (as alkalinity) (Spearman  $\text{DIC-alkalinity} = 0.89$ ).

Surface water primary production appears to have played a significant role in regulating  $\text{CO}_2$  levels in agricultural reservoirs, as DO levels were correlated negatively ( $P < 0.05$ ) with  $\text{CO}_2$  concentrations, as seen in other microbially-regulated systems (Cole & Caraco, 2001; Hanson et al., 2006; Stets et al., 2017; Vachon et al., 2020). Similarly, the strong negative relationship observed between  $\text{CO}_2$  and chlorophyll *a* is consistent with the role of autotrophs in regulating aquatic gas content (Figure 5), as observed previously in other agricultural reservoirs within this region (Webb et al., 2019b). The coupling of near-surface  $\text{CO}_2$  in reservoirs with  $\text{DOC:NO}_x$ , suggests that higher autotrophic activity depletes  $\text{NO}_x$  content in this N-limited region (Bergbusch et al., 2021; Gilbert et al., 2016; Swarbrick et al., 2019; Waiser et al., 2011).

### 4.3 Regulation of Methane Concentrations

Analysis with GAMs revealed that  $\text{CH}_4$  concentrations were correlated negatively to dissolved oxygen levels in reservoirs, suggesting the presence of anoxic methane production (Fig. 5; Megonigal et al., 2004, see also Bogard et al., 2014). In addition, we observed the lowest  $\text{CH}_4$  concentrations in reservoirs where  $\text{O}_2$  was supersaturated in surface waters. However, the lack of relationship between  $\text{CH}_4$  and deepwater DO may suggest that surface  $\text{CH}_4$  was more strongly impacted by consumption in the water column rather than production at depth (D'Ambrosio & Harrison, 2021; Hanson and Hanson, 1996, Holgerson et al., 2015,). As such, surface water  $\text{CH}_4$  concentration in the reservoirs appears to be regulated by  $\text{O}_2$  changes due to primary productivity. In contrast,  $\text{CH}_4$  levels

in wetland ponds were unrelated to DO content, suggesting insufficient time for gas oxidation before release to the atmosphere in these substantially shallower systems (Holgerson et al., 2015).

Stratification strength (as buoyancy frequency) was significant in GAMs for both reservoirs and wetlands, with a negative relationship with  $\text{CH}_4$  in reservoirs and positive relationship in wetlands (Fig. 5). The negative relationship in reservoirs is consistent with  $\text{CH}_4$  remaining trapped in the cool deep water, as seen elsewhere (Bastviken et al., 2004; Holgerson, 2015; Juutinen et al., 2009; Kankaala et al., 2013), possibly allowing for more oxidation in the water column (Saarela et al., 2020). In contrast, the positive relationship between stratification strength and  $\text{CH}_4$  levels seen in wetland ponds was unexpected, and may reflect a disproportionate effect of the seven thermally-stratified wetland ponds. Here, it may be that the very shallow wetland systems never stratify, and could simply exhibit more rapid equilibration with the atmosphere.

A negative relationship between  $\text{CH}_4$  and surface water conductivity in wetland ponds (Figure 5) suggests that sulfate-reducing bacteria may have outcompeted methanogenic bacteria for metabolic substrates. Surfacewater conductivity is highly correlated with sulfate concentrations (adj.  $R^2 = 0.83$ ) in these systems and previous analyses (Webb et al. unpublished data) show that sulfate concentrations (up to  $3883 \text{ mg L}^{-1}$  in reservoirs;  $6687 \text{ mg L}^{-1}$  in ponds) can be high enough to inhibit methanogenesis in freshwaters (Lovley & Klug, 1983). Similar negative relationships between  $\text{CH}_4$  concentrations and conductivity are known from other reservoirs in our study region (Webb et al., 2019b), as well as natural wetlands in North America and Europe (Gauci et al., 2004). Conductivity was also a significant predictor of  $\text{CH}_4$  in the reservoirs, however the relationship was unimodal with the lowest concentrations of  $\text{CH}_4$  observed at conductivity values of approximately  $1000 \text{ }\mu\text{S cm}^{-1}$ . In these deeper, more frequently stratified sites, then, it may be that inhibition of methanogenesis is not as strong a determinant of  $\text{CH}_4$  production as DO and stratification strength. Further research will be needed to resolve this issue.

The positive relationships between  $\text{DOC}:\text{NO}_x$ , chlorophyll *a*, and  $\text{CH}_4$  concentrations in agricultural reservoirs, but not wetland ponds, suggests that  $\text{CH}_4$  production may be limited by the supply of labile organic matter supply in constructed waterbodies. Alternately, this difference between reservoirs and ponds may be attributed to the age of the system - agricultural reservoirs are typically only a few decades old, and may not have as high as supply of DOC (Table 1) to form labile substrates for methanogens, while wetland ponds have large pools of DOC that is often refractory (Waiser and Robarts, 2004). While sediments were not sampled from either waterbody,  $\text{CH}_4$  levels are known to increase with sediment C content and C:N ratios in other regional agricultural reservoirs (Webb et al., 2019b), supporting this possible mechanism.

We found strong evidence that methane ebullition was inhibited by the presence of sulfate-reducing bacteria in both waterbody types (Fig. S3). Here, measured  $\text{CH}_4$  ebullition was inversely related to conductivity over nine ecosystems. Al-

though wetland ponds appeared to produce more  $\text{CH}_4$  bubbles than reservoirs at equivalent conductivity values, this pattern may arise because of higher DOC concentrations (Table 1) and more C-rich sediments favouring methanogenesis in the older wetland ponds (Colas et al., 2021). The mean ebullition rates estimated from the conductivity relationship in this study are comparable to ebullition rates observed in many other ecosystems (Table 2). The maximum ebullition estimate from natural wetland ponds ( $103.5 \text{ mmol m}^{-2} \text{ day}^{-1}$ ) is on the higher end of ebullition values observed in the literature. However, similar rates have been observed in a shallow eutrophic lake ( $96 \text{ mmol m}^{-2} \text{ day}^{-1}$ ; Martinez et al., 2013), and eutrophic urban ponds ( $82 \text{ mmol m}^{-2} \text{ day}^{-1}$ , Aben et al., 2017; Downing et al., 2012), with rates almost double (up to  $195 \text{ mmol m}^{-2} \text{ day}^{-1}$ ) observed in some rivers (Aben et al., 2017; Bastviken et al., 2011; Chen et al., 2021; Wang et al., 2021).

#### 4.4 Regulation of Nitrous Oxide Concentrations

On average,  $\text{N}_2\text{O}$  concentrations were undersaturated in both agricultural reservoirs and natural ponds, although wetlands were typically stronger  $\text{N}_2\text{O}$  sinks than were constructed waterbodies, in part reflecting outgassing from four reservoirs (Fig. 7; Table 1).  $\text{N}_2\text{O}$  concentrations were within the range seen in many lentic waterbodies (Table 2), with values below those characteristic of flowing waters (Webb et al., 2021). Specifically, prairie waterbodies sampled here had similar  $\text{N}_2\text{O}$  concentrations to those seen in other regional agricultural reservoirs (Webb et al., 2019a), small polymictic lakes in Ireland (Whitfield et al., 2011), small boreal lakes and reservoirs of varying trophic status in Finland (Huttunen et al., 2002; 2003), and boreal ponds in Canada (Soued et al., 2016). However, ours is the first study to report such a high proportion (~95%) of undersaturation among wetland ponds.

Despite similar in situ values,  $\text{N}_2\text{O}$  concentrations appeared to be regulated by different processes in small prairie ponds and constructed waterbodies (Fig. 6). In principle, production of  $\text{N}_2\text{O}$  arises from incomplete denitrification (Firestone and Davidson 1989), nitrification (Baulch et al. 2011a), and dissimilatory nitrate reduction to ammonium (DNRA; Scott et al. 2008), whereas complete denitrification is the only process known to consume  $\text{N}_2\text{O}$  (Quick et al., 2019). Each of these processes is affected by ecosystem productivity (Kemp and Dodds 2002), the presence of oxygen in specific habitats (e.g., shallow and deepwaters, sediments; Knowles, 1982), substrate concentrations (e.g., inorganic nitrogen; Kemp and Dodds, 2002; Taylor and Townsend, 2010), and their effects on consequent microbial activities (Taylor and Townsend 2010). Given that only denitrification is known to be capable of reducing  $\text{N}_2\text{O}$  levels (Quick et al. 2019), and that most prairie waters were undersaturated with  $\text{N}_2\text{O}$  (Fig. 7), we infer that differences in regulatory processes between constructed wetlands and natural ponds (Fig 6) reflect variation in the locale or intensity of denitrification, with more intense consumption of  $\text{N}_2\text{O}$  in natural wetland ecosystems.

In reservoirs, concentrations of  $\text{N}_2\text{O}$  exhibited positive relationships with the

degree of DO saturation,  $\text{NO}_x$  concentration, and DOC content, whereas  $\text{N}_2\text{O}$  levels declined with primary production, as Chl a (Fig. 6). Overall, these patterns are consistent with the predominant control operating via  $\text{N}_2\text{O}$  consumption through denitrification (Baulch et al. 2011a; Zhang et al., 2021), while the negative relationship with Chl a suggests competition between primary producers and  $\text{N}_2\text{O}$ -producing microbes for nitrogen species in agricultural reservoirs (Webb et al., 2019a). For example, elevated production in deep or stratified systems would be expected to lead to deepwater anoxia that favours complete denitrification and consumption of extant  $\text{N}_2\text{O}$ . The positive relationships between  $\text{N}_2\text{O}$  and  $\text{NO}_x$  may reflect  $\text{NO}_x$ -limited denitrification in the region (e.g. Gooding and Baulch 2017). Specifically, higher  $\text{N}_2\text{O}$  production via denitrification may occur where increased  $\text{NO}_x$  concentrations stimulate this process, or increase the  $\text{N}_2\text{O}$  yield of this process (Baulch et al. 2011b). Denitrification is also potentially stimulated by higher DOC (Knowles, 1982; Gooding and Baulch 2017), again consistent with relationships seen in reservoirs. Nitrification in reservoirs could also lead to the observed positive relationships between  $\text{N}_2\text{O}$  and  $\text{NO}_x$  via concurrent production of  $\text{NO}_x$  and  $\text{N}_2\text{O}$ . Nitrification is highly oxygen-sensitive, and may be stimulated by increased oxygen availability (e.g. Rysgaard et al. 1994; Kemp and Dodds 2002).

In contrast to results in reservoirs, in natural ponds,  $\text{N}_2\text{O}$  concentrations decreased as the DO saturation in surface waters increased,  $\text{NO}_x$  concentrations increased, and DOC content increased (Fig. 6). Ponds, with their shallower mean depth, may have a greater importance of benthic processes and also have high habitat heterogeneity, which may yield complex relationships, consistent with multiple drivers affecting N cycling and  $\text{N}_2\text{O}$  production.

The negative relationship between  $\text{N}_2\text{O}$  and DO in wetlands, and high degree of  $\text{N}_2\text{O}$  undersaturation in well oxygenated waters is novel. Typically,  $\text{N}_2\text{O}$  undersaturation in freshwaters is observed under low oxygen conditions (Zhang et al., 2021). In shallow productive environments such as our study ponds, these patterns may emerge due to diffusion between anoxic sediments and overlying habitats which are often highly productive. However, while anaerobic denitrification is traditionally the only known biological pathway of  $\text{N}_2\text{O}$  reduction, aerobic bacteria and cyanobacteria have been found to have the *NosZ* gene and are therefore capable of  $\text{N}_2\text{O}$  consumption (Farias et al., 2013; Park et al., 2017; Rees et al., 2021). Some have even found evidence of assimilative  $\text{N}_2\text{O}$  reduction into particulate organic nitrogen by marine cyanobacterial cultures (Farias et al., 2013) and biological  $\text{N}_2\text{O}$  consumption has been observed in oxygenated marine waters (Cornejo et al., 2015; Rees et al., 2021). To our knowledge, such strong  $\text{N}_2\text{O}$  undersaturation has not been observed before in highly oxygenated fresh waterbodies, hence it is also possible there is an alternative  $\text{N}_2\text{O}$  consumption mechanism that may be decoupled from  $\text{NO}_3$  reduction. Further experimentation will be required to evaluate the potential of this mechanism, as well as the relative importance of water column and sedimentary processes in controlling  $\text{N}_2\text{O}$  fluxes in small prairie waterbodies.



#### 4.5 CO<sub>2</sub>-equivalent fluxes

We found that wetland ponds were more frequently sinks of GHGs than were agricultural reservoirs (Fig. 8), although, on average, agricultural reservoirs contributed ~60% less CO<sub>2</sub> equivalent (CO<sub>2-eq</sub>) to the atmosphere than did natural wetlands (Figure 7D). Estimates of CO<sub>2-eq</sub> flux in this study showed that ~5% of agricultural reservoirs and ~15% of wetland ponds are acting as net CO<sub>2-eq</sub> sinks when calculated using the 100-year sustained-flux global warming and cooling potentials (Neubauer & Magonigal, 2015) (Figure 8). These proportions are similar to those reported for small agricultural reservoirs in Australia (Table 2), which found that the importance of individual GHG varied among CO<sub>2</sub> (55% of effect) CH<sub>4</sub> (42%) and N<sub>2</sub>O (3%) (Ollivier et al., 2019), despite the earlier study not reporting CH<sub>4</sub> ebullition which can account for up to 90% of total CH<sub>4</sub> emissions (Grinham et al., 2018a). Instead, CO<sub>2-eq</sub> fluxes observed in these waterbodies were comparable to other natural (Bortolotti et al. 2016; Kankaala et al. 2013; Whitfield et al., 2011) and constructed (Ollivier et al., 2018; 2019; Webb et al., 2019b) waterbodies, even though most previous studies do not include N<sub>2</sub>O fluxes and ebullitive CH<sub>4</sub> losses (Table 2).

Table 2. Flux values of carbon dioxide (CO<sub>2</sub>), methane (CH<sub>4</sub>), and nitrous oxide (N<sub>2</sub>O) recorded herein along with literature values. Diffusive flux values reported for CO<sub>2</sub>, CH<sub>4</sub>, N<sub>2</sub>O, while Ebullitive flux only reported for CH<sub>4</sub>. \* = mean value, \*\* = modeled value.

Citation	System	Region	CO <sub>2</sub> Diffu- sive mmol m <sup>-2</sup> day <sup>-1</sup>	CH <sub>4</sub> Diffu- sive mmol m <sup>-2</sup> day <sup>-1</sup>	N <sub>2</sub> O Diffu- sive μmol m <sup>-2</sup> day <sup>-1</sup>	CH <sub>4</sub> Ebulli- tion mmol m <sup>-2</sup> day <sup>-1</sup>
Ollivier et al. 2018	Agricultural Reser- voirs	Australia	to 30.24	to 10	-	-
Ollivier et al. 2019	Agricultural Reser- voirs	Australia	*	*	*	**
<b>Present Study</b>	<b>Agricultural Reser- voirs</b>	<b>Saskatchewan, Canada</b>	<b>30 to 464</b>	<b>0 to 13.5</b>	<b>-9.66 to 11.61</b>	<b>0.04 to 168.45**</b>
Webb et al. 2019a	Agricultural Reser- voirs	Saskatchewan, Canada		-	to 166	-
Webb et al. 2019b	Agricultural Reser- voirs	Saskatchewan, Canada	to 466	to 92	-	-

Peacock et al. 2021	Artificial Water- bodies	Sweden	*	*	-	*
D'Acunha and Johnson 2019	Constructed Stormwa- ter Wet- lands	British Columbia, Canada	to 1266	to 55.5	to 57.47	-
McClure et al. 2020	Eutrophic Reser- voir	North America	-	to 1.37	-	to 2.24
Jeffrey et al. 2019	Freshwater Subtrop- ical Wetland	Australia	-	to 66.2	-	*
Bastviken et al. 2004	Lakes	North America	-	to 0.43	-	to 2.79
DelSontro et al. 2016	Lakes	Quebec, Canada	*	*	-	*
Strayer and Tiedje 1978	Lakes	North America	-	to 46	-	*
Bortolotti et al. 2016	Natural and Re- stored Wetland Ponds	Saskatchewan, Canada	to 1,1350	to 13.3	-	-
<b>Present Study</b>	<b>Natural Wet- land Ponds</b>	<b>Saskatchewan, Canada</b>	<b>to 784</b>	<b>0.13 to 14.11</b>	<b>-13.5 to 2.2</b>	<b>0.002 to 4657.6**</b>
DelSontro et al. 2016	Ponds	Quebec, Canada	*	*	-	*
Huttunen et al. 2002	Ponds	Finland	to 2.50	to 4.55	to 3.86	-
Badiou et al. 2011	Prairie Wetland Ponds	Prairie Pothole Region, Canada	-	to 3.81	to 20.0	-

McNicol et al. 2017	Restored Wetland	California, USA	to 3773	to 7.42	to 103.68	to 2.3
Natchimuth et al. 2014	Shallow Ponds	Sweden	to 16.0	to 13.1	-	to 11.6
Grinham et al. 2018b	Small Artificial Water-bodies	Australia	-	< 3.12	-	> 3.12
Whitfield et al. 2011	Small Headwater Lakes	Ireland	to 46	to 4.5	to 6.9	-
Repo et al. 2007	Small Wetland Lakes	Siberia	to 84.07	to 7.48	-	to 0.686
Yang et al. 2015	Subtropical Aquaculture Ponds	China	to 50.9	to 141.9	to 17.72	-
Villa et al. 2021	Temperate Freshwater Marsh	Ohio, USA	-	*	-	to 95.04
Prėskienis et al. 2021	Tundra Lakes and Ponds	Nunavut, Canada	to 23.39	to 0.955	-	to 5.255
van Bergen et al. 2019	Urban Pond	Netherlands*		*	-	*
Panneer Selvam et al. 2014	Various Inland Waters	India	to 253.2	*	-	*

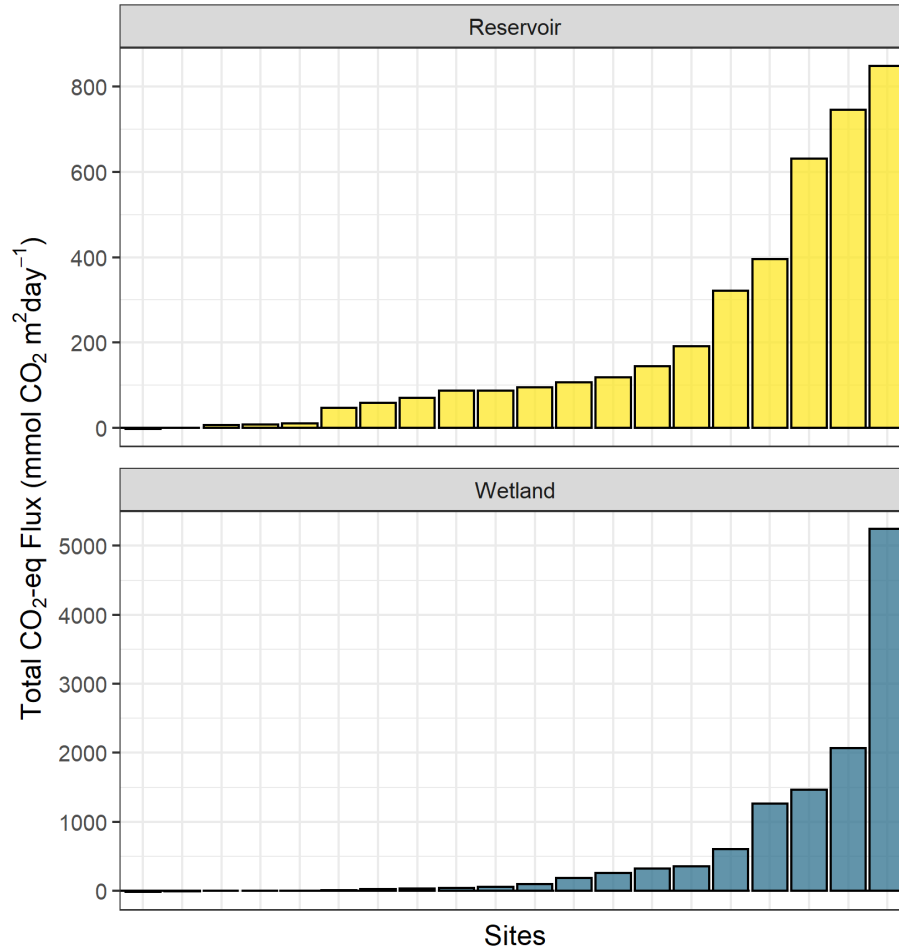


Figure 8. Total carbon dioxide (CO<sub>2</sub>)-equivalent flux from each reservoir (top) and wetland (bottom). All values include diffusive flux from carbon dioxide, methane, and nitrous oxide, as well as ebullitive methane flux predicted from water conductivity. Carbon dioxide equivalence calculated using the 100-year sustained global warming and cooling potentials (Neubauer & Megonigal, 2015). Each bar represents one site. One reservoir and three wetlands are net CO<sub>2</sub> sinks. Note difference in y-axis scale.

In the context of up-scaling of carbon budgets for inland waters (Cole et al., 2007; Tranvik et al., 2009), our results present a novel finding that CO<sub>2</sub> and CH<sub>4</sub> fluxes are comparable between natural wetland ponds and constructed agricultural reservoirs, whereas N<sub>2</sub>O fluxes are significantly lower in natural wetland ponds. This result combined with the finding that the mechanisms controlling the production and consumption of GHGs appear to differ between these waterbody types suggests that landscape models of integrated GHG flux

should distinguish between natural and artificial waterbodies. We also conclude that natural and artificial waterbodies of similar sizes may exhibit substantially different regulatory mechanisms and that artificial waterbodies should have their own recognition in emission factor models, as suggested by Webb et al. (2021). Given that ponds and reservoirs were co-located in similar landscapes, we infer that the overarching differences in GHG dynamics between waterbody types may be driven mainly by differences in morphology, stratification and age of the two basins, factors which affect pond mixing, nutrient content, and ecosystem productivity.

#### Acknowledgments, Samples, and Data

**Data availability:** All data and R code is available online in a GitHub repository ([https://github.com/finlay4k/Jensen\\_wetland\\_dugout.git](https://github.com/finlay4k/Jensen_wetland_dugout.git)). Public access to this repository will be made available upon publication and a DOI will be generated at that time.

**Supplement:** The supporting information related to this study will be published online.

**Author contributions:** S.A.J., J.R.W., G.L.S., P.R.L., H.M.B., and K.F. designed research; S.A.J. performed research and wrote the paper; H.M.B. contributed new reagents/analytic tools; J.R.W., P.R.L., G.L.S., H.M.B. and K.F. contributed towards ideas and data analysis; S.A.J. developed generalized additive models. All authors revised and approved the final manuscript.

**Competing interests:** The authors declare no competing interests

**Acknowledgements:** Financial support for data collection and analyses were provided in part by Government of Saskatchewan (Award 200160015), Natural Sciences and Engineering Research Council of Canada Discovery grants (to K.F., G.L.S., H.M.B., and P.R.L.), the Canada Foundation for Innovation, University of Regina. . We thank Shaeya Cluff, Ann King, and Mackenzie Metz for field-work assistant and all landowners for their generous cooperation in volunteering their reservoirs for this research. This research took place on Treaty 4 and 6 territories, traditional areas of Cree, Saulteaux, Lakota, Dakota, and Nakota peoples, and homeland of the Métis.

#### References

- Badiou, P., McDougal, R., Pennock, D., & Clark, B. (2011). Greenhouse gas emissions and carbon sequestration potential in restored wetlands of the Canadian prairie pothole region. *Wetlands Ecology and Management*, 19, 237-256. <https://doi.org/10.1007/s11273-011-9214-6>
- Bastviken, D., Cole, J., Pace, M., & Tranvik, L. (2004). Methane emissions from lakes: Dependence of lake characteristics, two regional assessments, and a global estimate. *Global Biogeochemical Cycles*, 18(4), GB4009. <https://doi.org/10.1029/2004gb002238>

- Baulch, H., Dillon, P., Maranger, R., & Schiff, S. (2011a). Diffusive and ebullitive transport of methane and nitrous oxide from streams: Are bubble-mediated fluxes important?. *Journal of Geophysical Research: Biogeosciences*, 116, G04028. <https://doi.org/0.1029/2011JG001656>
- Baulch, H.M., S.L. Schiff, R. Marager, & P.J. Dillon. (2011b). Nitrogen enrichment and the emission of nitrous oxide from streams. *Global Biogeochemical Cycles*. <https://doi.org/10.1029/2011GB004047>
- Baulch, H., C. Whitfield, J. Wolfe, N. Basu, A. Bedard-Haughn, K. Belcher, R. Clark, G. Ferguson, M. Hayashi, A. Ireson, P. Lloyd-Smith, P. Loring, J.W. Pomeroy, K. Shook, C. Spence. 2021. Synthesis of science: findings on Canadian Prairie wetland drainage. *Canadian Water Resources Journal*. <https://doi.org/10.1080/07011784.2021.1973911>
- Bernhardt, E., & Likens, G. (2002). Dissolved organic carbon enrichment alters nitrogen dynamics in a forest stream. *Ecology*, 83(6), 1689-1700. [https://doi.org/10.1890/0012-9658\(2002\)083\[1689:DOCEAN\]2.0.CO;2](https://doi.org/10.1890/0012-9658(2002)083[1689:DOCEAN]2.0.CO;2)
- Bogard, M. J., Finlay, K., Waiser, M. J., Tumber, V. P., Donald, D. B., Wiik, E., et al. (2017). Effects of experimental nitrogen fertilization on planktonic metabolism and CO<sub>2</sub> flux in a hypereutrophic hardwater lake. *PLoS ONE*, 12(12), e0188652. <https://doi.org/10.1371/journal.pone.0188652>
- Bogard, M. J., Giorgio, P. A. del, Boutet, L., Chaves, M. C. G., Prairie, Y. T., Merante, A., & Derry, A. M. (2014). Oxic water column methanogenesis as a major component of aquatic CH<sub>4</sub> fluxes. *Nature Communications*, 5, 5350. <https://doi.org/10.1038/ncomms6350>
- Bortolotti, L. E., St. Louis, V.L., Vinebrooke, R.D., & Wolfe, A.P. (2016). Net Ecosystem Production and Carbon Greenhouse Gas Fluxes in Three Prairie Wetlands. *Ecosystems*, 19, 411-425. <https://doi.org/10.1007/s10021-015-9942-1>
- Bridgman, S. D., Cadillo-Quiroz, H., Keller, J. K., & Zhuang, Q. (2013). Methane emissions from wetlands: biogeochemical, microbial, and modeling perspectives from local to global scales. *Global Change Biology*, 19, 1325-1346. <https://doi.org/10.1111/gcb.12131>
- Clifford, C. C., & Heffernan, J. B. (2018). Artificial Aquatic Ecosystems. *Water*, 10, 1096. <https://doi.org/10.3390/w10081096>
- Colas, F., Baudoin, J.M., Bonin, P., Cabrol, L., Daufresne, M., Lassus, R., & Cucherousset, J. (2021). Ecosystem maturity modulates greenhouse gases fluxes from artificial lakes. *Science of The Total Environment*, 760, 144046. <https://doi.org/10.1016/j.scitotenv.2020.144046>
- Cole, J. J., & Caraco, N. F. (1998). Atmospheric exchange of carbon dioxide in a low-wind oligotrophic lake measured by the addition of SF<sub>6</sub>. *Limnology and Oceanography*, 43(4), 647-656. <https://doi.org/10.4319/lo.1998.43.4.0647>

- Cole, J. J., & Caraco, N. F. (2001). Carbon in catchments: connecting terrestrial carbon losses with aquatic metabolism. *Marine and Freshwater Research*, 52, 101–110. <https://doi.org/10.1071/mf00084>
- Cole, J., Prairie, Y., Caraco, N., McDowell, W., Tranvik, L., Striegl, R., et al. (2007). Plumbing the Global Carbon Cycle: Integrating Inland Waters into the Terrestrial Carbon Budget. *Ecosystems*, 10, 171–184. <https://doi.org/10.1007/s10021-006-9013-8>
- Cornejo, M., A.A. Murillo, & L. Farias. (2015). An unaccounted for N<sub>2</sub>O sink in the surface water of the eastern subtropical South Pacific: Physical versus biological mechanisms. *Progress in Oceanography*, 137: 12–23. <https://doi.org/10.1016/j.pocean.2014.12.016>
- Cortus, B. G., Jeffrey, S. R., Unterschultz, J. R., & Boxall, P. C. (2011). The Economics of Wetland Drainage and Retention in Saskatchewan. *Canadian Journal of Agricultural Economics*, 59, 109–126. <https://doi.org/10.1111/j.1744-7976.2010.01193.x>
- D’Ambrosio, S. & Harrison, J.A. (2021). Methanogenesis exceeds CH<sub>4</sub> consumption in eutrophic lake sediments. *Limnology and Oceanography Letters*, 6, 173–181. <https://doi.org/10.1002/lol2.10192>
- D’Acunha, B., & Johnson, M. S. (2019). Water quality and greenhouse gas fluxes for stormwater detained in a constructed wetland. *Journal of Environmental Management*, 231, 1232–1240. <https://doi.org/10.1016/j.jenvman.2018.10.106>
- Davidson, T. A., Audet, J., Svenning, J., Lauridsen, T. L., Søndergaard, M., Landkildehus, F., et al. (2015). Eutrophication effects on greenhouse gas fluxes from shallow-lake mesocosms override those of climate warming. *Global Change Biology*, 21, 4449–4463. <https://doi.org/10.1111/gcb.13062>
- Deemer, B. R., Harrison, J. A., Li, S., Beaulieu, J. J., DelSontro, T., Barros, N., et al. (2016). Greenhouse Gas Emissions from Reservoir Water Surfaces: A New Global Synthesis. *BioScience*, 66(11), 949–964. <https://doi.org/10.1093/biosci/biw117>
- DelSontro, T., Boutet, L., St-Pierre, A., Giorgio, P., & Prairie, Y. (2016). Methane ebullition and diffusion from northern ponds and lakes regulated by the interaction between temperature and system productivity. *Limnology and Oceanography*, 61, S62–S77. <https://doi.org/10.1002/lno.10335>
- Downing, J. (2010). Emerging global role of small lakes and ponds: little things mean a lot. *Limnetica*, 29(1), 9–24.
- Downing, J. A., Prairie, Y. T., Cole, J. J., Duarte, C. M., Tranvik, L. J., Striegl, R. G., et al. (2006). The global abundance and size distribution of lakes, ponds, and impoundments. *Limnology and Oceanography*, 51(5), 2388–2397. <https://doi.org/10.4319/lo.2006.51.5.2388>
- Duarte, C. M., Prairie, Y. T., Montes, C., Cole, J. J., Striegl, R., Melack, J., &

- Downing, J. A. (2008). CO<sub>2</sub> emissions from saline lakes: A global estimate of a surprisingly large flux. *Journal of Geophysical Research: Biogeosciences*, 113, G04041. <https://doi.org/10.1029/2007jg000637>
- Euliss, N. H., Mushet, D. M., & Wrubleski, D. A. (1999). Wetlands of the Prairie Pothole Region: Invertebrate species composition, ecology, and management. In D. P. Batzer, R. R. B., & W. S. A. (Eds.), *Invertebrates in freshwater wetlands of North America: ecology and management* (pp. 471–514). New York: Wiley.
- Farías, L. J. Faúndex, C. Fernándex, M. Cornejo, S. Sanhueza, & C. Carrasco. (2013). Biological N<sub>2</sub>O fixation in the eastern south Pacific Ocean and marine cyanobacterial cultures. *PLOS One*, 8(5), e63956. <https://doi.org/10.1371/journal.pone.0063956>
- Finlay, K., Leavitt, P., Wissel, B., & Prairie, Y. (2009). Regulation of spatial and temporal variability of carbon flux in six hard-water lakes of the northern Great Plains. *Limnology and Oceanography*, 54(6part2), 2553-2564. [https://doi.org/10.4319/lo.2009.54.6\\_part\\_2.2553](https://doi.org/10.4319/lo.2009.54.6_part_2.2553)
- Finlay, K., Vogt, R., Bogard, M., Wissel, B., Tutolo, B., Simpson, G., & Leavitt, P. (2015). Decrease in CO<sub>2</sub> efflux from northern hardwater lakes with increasing atmospheric warming. *Nature*, 519, 215-218. <https://doi.org/10.1038/nature14172>
- Firestone, M.K., & Davidson, E.A. 1989. Microbiological basis of NO and N<sub>2</sub>O production and consumption in soil. Exchange of Trace Gases between Terrestrial Ecosystems and the Atmosphere. Eds M.O. Andreae and D.S. Schimel. Pp 7-21. Wiley and Sons.
- Galy-Lacaux, C., Delmas, R., Kouadio, G., Richard, S., & Gosse, P. (1999). Long-term greenhouse gas emissions from hydroelectric reservoirs in tropical forest regions. *Global Biogeochemical Cycles*, 13(2), 503–517. <https://doi.org/10.1029/1998gb900015>
- Gauci, V., Matthews, E., Dise, N., Walter, B., Koch, D., Granberg, G., & Vile, M. (2004). Sulfur pollution suppression of the wetland methane source in the 20th and 21st centuries. *Proceedings of the National Academy of Sciences of the United States of America*, 101(34), 12583–12587. <https://doi.org/10.1073/pnas.0404412101>
- Glibert, P. M., Wilkerson, F.P., Dugdale, R. C., Raven, J.A., Dupont, C. L., Leavitt, P. R., et al. (2016). Pluses and minuses of ammonium and nitrate uptake and assimilation by phytoplankton and implications for productivity and community composition, with emphasis on nitrogen-enriched conditions. *Limnology and Oceanography*, 61, 165–197. <http://doi.org/10.1002/lno.10203>
- Gooding, R.M., & H.M. Baulch. (2017). Small reservoirs as beneficial management practice for nitrogen removal. *Journal of Environmental Quality*, 46, 96-104. <https://doi.org/10.2134/jeq2016.07.0252>



- Grinham, A., Albert, S., Deering, N., Dunbabin, M., Bastviken, D., Sherman, B., et al. (2018). The importance of small artificial water bodies as sources of methane emissions in Queensland, Australia. *Hydrology and Earth System Sciences*, 22(10), 5281–5298. <https://doi.org/10.5194/hess-22-5281-2018>
- Grinham, A., Dunbabin, M., & Albert, S. (2018). Importance of sediment organic matter to methane ebullition in a sub-tropical freshwater reservoir. *Science of The Total Environment*, 621, 1199–1207. <https://doi.org/10.1016/j.scitotenv.2017.10.108>
- Hanson, P. C., Carpenter, S. R., Armstrong, D. E., Stanley, E. H., & Kratz, T. K. (2006). Lake dissolved inorganic carbon and dissolved oxygen: changing drivers from days to decades. *Ecological Monographs*, 76(3), 343–363. [https://doi.org/10.1890/0012-9615\(2006\)076\[0343:ldicad\]2.0.co;2](https://doi.org/10.1890/0012-9615(2006)076[0343:ldicad]2.0.co;2)
- Hanson, R. S., & Hanson, T. E. (1996). Methanotrophic Bacteria. *Microbiological Reviews*, 60(2), 439–471. <https://doi.org/10.1128/mmbr.60.2.439-471.1996>
- Hayes, N. M., Deemer, B. R., Corman, J. R., Razavi, N. R., & Strock, K. E. (2017). Key differences between lakes and reservoirs modify climate signals: A case for a new conceptual model. *Limnology and Oceanography Letters*, 2(2), 47–62. <https://doi.org/10.1002/lol2.10036>
- Holgerson, M. (2015). Drivers of carbon dioxide and methane supersaturation in small, temporary ponds. *Biogeochemistry*, 124, 305–318. <https://doi.org/10.1007/s10533-015-0099-y>
- Holgerson, M., & Raymond, P. (2016). Large contribution to inland water CO<sub>2</sub> and CH<sub>4</sub> emissions from very small ponds. *Nature Geoscience*, 9(3), 222–226. <https://doi.org/10.1038/ngeo2654>
- Huttunen, J., Alm, J., Liikanen, A., Juutinen, S., Larmola, T., Hammar, T., et al. (2003). Fluxes of methane, carbon dioxide and nitrous oxide in boreal lakes and potential anthropogenic effects on the aquatic greenhouse gas emissions. *Chemosphere*, 52(3), 609–621. [https://doi.org/10.1016/S0045-6535\(03\)00243-1](https://doi.org/10.1016/S0045-6535(03)00243-1)
- Huttunen, J., Väisänen, T., Heikkinen, M., Hellsten, S., Nykänen, H., Nenonen, O., & Martikainen, P. (2002). Exchange of CO<sub>2</sub>, CH<sub>4</sub> and N<sub>2</sub>O between the atmosphere and two northern boreal ponds with catchments dominated by peatlands or forests. *Plant and Soil*, 242(1), 137–146. <https://doi.org/10.1023/A:1019606410655>
- Jeffrey, L. C., Maher, D. T., Johnston, S. G., Kelaher, B. P., Steven, A., & Tait, D. R. (2019). Wetland methane emissions dominated by plant-mediated fluxes: Contrasting emissions pathways and seasons within a shallow freshwater subtropical wetland. *Limnology and Oceanography*, 64(5), 1895–1912. <https://doi.org/10.1002/lno.11158>
- Jeffrey, S. W., & Humphrey, G. F. (1975). New spectrophotometric equations for determining chlorophylls a, b, c1 and c2 in higher plants, algae and natu-

- ral phytoplankton. *Biochemie Und Physiologie Der Pflanzen*, 167(2), 191–194. [https://doi.org/10.1016/s0015-3796\(17\)30778-3](https://doi.org/10.1016/s0015-3796(17)30778-3)
- Jensen, S. A. (2021). Magnitude and Regulating Factors of Carbon Dioxide, Methane, and Nitrous Oxide Concentrations From Natural and Constructed Agricultural Waterbodies on the Northern Great Plains, (Master’s thesis). Regina, SK: University of Regina
- Joyce, J., & Jewell, P. W. (2003). Physical Controls on Methane Ebullition from Reservoirs and Lakes. *Environmental and Engineering Geoscience*, 9(2), 167–178. <https://doi.org/10.2113/9.2.167>
- Juutinen, S., Rantakari, M., Kortelainen, P., Huttunen, J. T., Larmola, T., Alm, J., et al. (2009). Methane dynamics in different boreal lake types. *Biogeosciences*, 6(2), 209–223. <https://doi.org/10.5194/bg-6-209-2009>
- Kalff, J., & Downing, J. A. (2016). *Limnology: Inland Water Ecosystems* (2nd ed.). Bibliogenica.
- Kankaala, P., Huotari, J., Tulonen, T., & Ojala, A. (2013). Lake-size dependent physical forcing drives carbon dioxide and methane effluxes from lakes in a boreal landscape. *Limnology and Oceanography*, 58(6), 1915–1930. <https://doi.org/10.4319/lo.2013.58.6.1915>
- Kemp, M.J. & W.K. Dodds. (2002). The influence of ammonium, nitrate, and dissolved oxygen concentrations on uptake, nitrification, and denitrification rates associated with prairie stream substrata. *Limnology and Oceanography*. <https://doi.org/10.4319/lo.2002.47.5.1380>
- Keller, M., & Stallard, R. F. (1994). Methane emission by bubbling from Gatun Lake, Panama. *Journal of Geophysical Research*, 99(D4), 8307–8319. <https://doi.org/10.1029/92jd02170>
- Knowles, R. 1982. Denitrification. *Microbiol. Rev.* 46(1): 43-70.
- Liikanen, A., Huttunen, J. T., Karjalainen, S. M., Heikkinen, K., Väisänen, T. S., Nykänen, H., & Martikainen, P. J. (2006). Temporal and seasonal changes in greenhouse gas emissions from a constructed wetland purifying peat mining runoff waters. *Ecological Engineering*, 26, 241–251. <https://doi.org/10.1016/j.ecoleng.2005.10.005>
- Lovley, D. R., & Klug, M. J. (1983). Sulfate reducers can outcompete methanogens at freshwater sulfate concentrations. *Applied and Environmental Microbiology*, 45(1), 187–192. <https://doi.org/10.1128/aem.45.1.187-192.1983>
- Maher, D. T., Call, M., Macklin, P., Webb, J.R., & Santos, I.R. (2019). Hydrological Versus Biological Drivers of Nutrient and Carbon Dioxide Dynamics in a Coastal Lagoon. *Estuaries and Coasts*, 42, 1015–1031. <https://doi.org/10.1007/s12237-019-00532-2>
- Marra, G., & S. N. Wood. (2011). Practical variable selection for generalized additive models. *Computational Statistics and Data Analysis*, 55, 2372–2387.

<https://doi.org/10.1016/j.csda.2011.02.004>

McClure, R. P., Lofton, M. E., Chen, S., Krueger, K. M., Little, J. C., & Carey, C. C. (2020). The Magnitude and Drivers of Methane Ebullition and Diffusion Vary on a Longitudinal Gradient in a Small Freshwater Reservoir. *Journal of Geophysical Research: Biogeosciences*, 125(3), e2019JG00520. <https://doi.org/10.1029/2019jg005205>

McNicol, G., Sturtevant, C., Knox, S., Dronova, I., Baldocchi, D., & Silver, W. (2017). Effects of seasonality, transport pathway, and spatial structure on greenhouse gas fluxes in a restored wetland. *Global Change Biology*, 23, 2768–2782. <https://doi.org/10.1111/gcb.13580>

Megonigal, J. P., Hines, M. E., & Visscher, P. T. (2004). Anaerobic metabolism: linkages to trace gases and aerobic processes. In W. H. Schlesinger (Ed.), *Biogeochemistry* (pp. 317–424). Oxford, UK: Elsevier-Pergamon.

Monteith, D. T., Evans, C. D., Henrys, P. A., Simpson, G. L., & Malcolm, I. A. (2014). Trends in the hydrochemistry of acidsensitive surface waters in the UK 1988–2008. *Ecological Indicators*, 37, 287–303. <http://dx.doi.org/10.1016/j.ecolind.2012.08.013>

Natchimuthu, S., Panneer Selvam, B., & Bastviken, D. (2014). Influence of weather variables on methane and carbon dioxide flux from a shallow pond. *Biogeochemistry*, 119, 403–413. <https://doi.org/10.1007/s10533-014-9976-z>

Neubauer, S. C., & Megonigal, J. P. (2015). Moving Beyond Global Warming Potentials to Quantify the Climatic Role of Ecosystems. *Ecosystems*, 18, 1000–1013. <https://doi.org/10.1007/s10021-015-9879-4>

Ollivier, Q. R., Maher, D. T., Pitfield, C., & Macreadie, P. I. (2018). Punching above their weight: Large release of greenhouse gases from small agricultural dams. *Global Change Biology*, 25, 721–732. <https://doi.org/10.1111/gcb.14477>

Ollivier, Q. R., Maher, D. T., Pitfield, C., & Macreadie, P. I. (2019). Winter emissions of CO<sub>2</sub>, CH<sub>4</sub>, and N<sub>2</sub>O from temperate agricultural dams: fluxes, sources, and processes. *Ecosphere*, 10(11), e02914. <https://doi.org/10.1002/ecs2.2914>

Orr, H. G., Simpson, G.L., des Clers, S., Watts, G., Hughes, M., Hannaford, J., et al. (2015). Detecting changing river temperatures in England and Wales. *Hydrological Processes*, 29, 752–766. <https://doi.org/10.1002/hyp.10181>

Panneer Selvam, B., Natchimuthu, S., Arunachalam, L., & Bastviken, D. (2014). Methane and carbon dioxide emissions from inland waters in India – implications for large scale greenhouse gas balances. *Global Change Biology*, 20, 3397–3407. <https://doi.org/10.1111/gcb.1257>

Park, D., Kim, H., & Yoon, S. (2017). Nitrous oxide reduction by an obligate aerobic bacterium *Gemmatimonas aurantiaca* Strain T-27. *Applied and Environmental Microbiology*, 83(12), e00502-17. <https://doi.org/10.1128/AEM.00502-17>

- Peacock, M., Audet, J., Bastviken, D., Cook, S., Evans, C. D., Grinham, A., et al. (2021). Small artificial waterbodies are widespread and persistent emitters of methane and carbon dioxide. *Global Change Biology*, 27, 5109–5123. <https://doi.org/10.1111/gcb.15762>
- Prėskienis, V., Laurion, I., Bouchard, F., Douglas, P. M. J., Billett, M. F., Fortier, D., & Xu, X. (2021). Seasonal patterns in greenhouse gas emissions from lakes and ponds in a High Arctic polygonal landscape. *Limnology and Oceanography*, 66, S117–S141. <https://doi.org/10.1002/lno.11660>
- Qin, B., Zhou, J., Elser, J. J., Gardner, W. S., Deng, J., & Brookes, J. D. (2020). Water Depth Underpins the Relative Roles and Fates of Nitrogen and Phosphorus in Lakes. *Environmental Science & Technology*, 54, 3191–3198. <https://doi.org/10.1021/acs.est.9b05858>
- Quick, A. M., Reeder, W. J., Farrell, T. B., Tonina, D., Feris, K. P., & Benner, S. G. (2019). Nitrous oxide from streams and rivers: A review of primary biogeochemical pathways and environmental variables. *Earth-Science Reviews*, 191, 224–262. <https://doi.org/10.1016/j.earscirev.2019.02.021>
- R Core Team. (2021). R: a language and environment for statistical computing; <https://www.R-project.org/>
- Read, J. S., Hamilton, D. P., Desai, A. R., Rose, K. C., MacIntyre, S., Lenters, J. D., et al. (2012). Lake-size dependency of wind shear and convection as controls on gas exchange. *Geophysical Research. Letters*, 39, L09405. <https://doi.org/10.1029/2012GL051886>
- Rees, A. P., Brown, I. J., Jayakumar, A., Lessin, G., Somerfield, P. J., & Ward, B. B. (2021). Biological nitrous oxide consumption in oxygenated waters of the high latitude Atlantic Ocean. *Communications Earth & Environment*, 2(1), 36. <https://doi.org/10.1038/s43247-021-00104-y>
- Repo, M., Huttunen, J., Naumov, A., Chichulin, A., Lapshina, E., Bleuten, W., & Mikainen, P. (2007). Release of CO<sub>2</sub> and CH<sub>4</sub> from small wetland lakes in western Siberia. *Tellus B*, 59B, 788–796. <https://doi.org/10.1111/j.1600-0889.2007.00301.x>
- Rysgaard, S., N. Risgaard-Petersen, S.N. Peter, J. Kim, N.L. Peter. (1994). Oxygen regulation of nitrification and denitrification in sediments. *Limnology and Oceanography*. <https://doi.org/10.4319/lo.1994.39.7.1643>
- Saarela, T., Rissanen, A. J., Ojala, A., Pumpanen, J., Aalto, S. L., Tirola, M., et al. (2020). CH<sub>4</sub> oxidation in a boreal lake during the development of hypolimnetic hypoxia. *Aquatic Sciences*, 82(2), 19. <https://doi.org/10.1007/s00027-019-0690-8>
- Scott, J.T., McCarthy, M.J., Gardner, W.S., Doyle, R.D. 2008. Denitrification, dissimilatory nitrate reduction to ammonium, and nitrogen fixation along a nitrate concentration gradient in a created freshwater wetland. *Biogeochemistry*, 87, 99–111. <https://doi.org/10.1007/s10533-007-9171-6>

- Soued, C., Giorgio, P. A. del, & Maranger, R. (2016). Nitrous oxide sinks and emissions in boreal aquatic networks in Québec. *Nature Geoscience*, 9, 116–120. <https://doi.org/10.1038/ngeo2611>
- Stets, E. G., Butman, D., McDonald, C. P., Stackpoole, S. M., DeGrandpre, M. D., & Striegl, R. G. (2017). Carbonate buffering and metabolic controls on carbon dioxide in rivers. *Global Biogeochemical Cycles*, 31, 663–677. <https://doi.org/10.1002/2016gb005578>
- Strayer, R. F., & Tiedje, J. M. (1978). In situ methane production in a small, hypereutrophic, hard-water lake: Loss of methane from sediments by vertical diffusion and ebullition. *Limnology and Oceanography*, 23(6), 1201–1206. <https://doi.org/10.4319/lo.1978.23.6.1201>
- Stumm, W., & Morgan, J. J. (1970). *Aquatic chemistry; an introduction emphasizing chemical equilibria in natural waters*. Wiley.
- Swarbrick, V. J., Simpson, G. L., Glibert, P. M., & Leavitt, P. R. (2019). Differential stimulation and suppression of phytoplankton growth by ammonium enrichment in eutrophic hardwater lakes over 16 years. *Limnology and Oceanography*, 64, S130–S149. <https://doi.org/10.1002/lno.11093>
- Swarbrick, V.J., N.T. Bergbusch, and P.R. Leavitt. 2022. Spatial and temporal patterns of urea content in a eutrophic stream continuum on the Northern Great Plains. *Biogeochemistry*, 157, 171–191. [doi.org/10.1007/s10533-021-00868-7](https://doi.org/10.1007/s10533-021-00868-7)
- Taylor, P.G., & A.R. Townsend. (2010). Stoichiometric control of organic carbon-nitrate relationships from soils to the sea. *Nature Letters* 464. <https://doi.org/10.1038/nature08985>
- Tian H, Lu, C., Ciais, P., Michalak, A. M., Canadell, J. G., Saikawa, E., et al. (2016) The terrestrial biosphere as a net source of greenhouse gases to the atmosphere. *Nature*, 531, 225–228. <https://doi.org/10.1038/nature16946>
- Tranvik, L., Downing, J., Cotner, J., Loiselle, S., Striegl, R., Ballatore, T., et al. (2009). Lakes and reservoirs as regulators of carbon cycling and climate. *Limnology and Oceanography*, 54(6, part 2), 2298–2314. [https://doi.org/10.4319/lo.2009.54.6\\_part\\_2.2298](https://doi.org/10.4319/lo.2009.54.6_part_2.2298)
- Vachon, D., Sadro, S., Bogard, M. J., Lapierre, J., Baulch, H. M., Rusak, J. A., et al. (2020). Paired O<sub>2</sub>–CO<sub>2</sub> measurements provide emergent insights into aquatic ecosystem function. *Limnology and Oceanography Letters*, 5(4), 287–294. <https://doi.org/10.1002/lol2.10135>
- van Bergen, T. J. H. M., Barros, N., Mendonca, R., Aben, R. C. H., Althuisen, I. H. J., Huszar, V., et al. (2019). Seasonal and diel variation in greenhouse gas emissions from an urban pond and its major drivers. *Limnology and Oceanography*, 64, 2129–2139. <https://doi.org/10.1002/lno.11173>
- Villa, J. A., Ju, Y., Yazbeck, T., Waldo, S., Wrighton, K. C., & Bohrer, G. (2021). Ebullition dominates methane fluxes from the water surface across

- different ecohydrological patches in a temperate freshwater marsh at the end of the growing season. *Science of The Total Environment*, 767, 144498. <https://doi.org/10.1016/j.scitotenv.2020.144498>
- Waiser, M.J., & Robarts, R.D. (2004). Photodegradation of DOC in a shallow prairie wetland: evidence from seasonal changes in DOC optical properties and chemical characteristics. *Biogeochemistry*, 69, 263– 284. <https://doi.org/10.1023/B:BIOG.0000031048.20050.4e>
- Waiser, M. J., V. Tumber, & J. Holm. (2011). Effluent dominated streams. Part 1: Presence and effects of excess nitrogen and phosphorus in Wascana Creek, Saskatchewan. Canada. *Environmental Toxicology and Chemistry* 30(2), 496–507. <https://doi.org/10.1002/etc.399>
- Webb, J. R., Clough, T. J., & Quayle, W. C. (2021). A review of indirect N<sub>2</sub>O emission factors from artificial agricultural waters. *Environmental Research Letters*, 16(4), 043005. <https://doi.org/10.1088/1748-9326/abed00>
- Webb, J. R., Hayes, N. M., Simpson, G. L., Leavitt, P. R., Baulch, H. M., & Finlay, K. (2019a). Widespread nitrous oxide undersaturation in farm waterbodies creates an unexpected greenhouse gas sink. *Proceedings of the National Academy of Sciences*, 116(20), 9814–9819. <https://doi.org/10.1073/pnas.1820389116>
- Webb, J. R., Leavitt, P. R., Simpson, G. L., Baulch, H. M., Haig, H. A., Hodder, K. R., & Finlay, K. (2019b). Regulation of carbon dioxide and methane in small agricultural reservoirs: optimizing potential for greenhouse gas uptake. *Biogeosciences*, 16(21), 4211–4227. <https://doi.org/10.5194/bg-16-4211-2019>
- Weiss, R. F. (1974). Carbon dioxide in water and seawater: the solubility of a non-ideal gas. *Marine Chemistry*, 2, 203–215. [https://doi.org/10.1016/0304-4203\(74\)90015-2](https://doi.org/10.1016/0304-4203(74)90015-2)
- Weiss, R. F., & Price, B. A. (1980). Nitrous oxide solubility in water and seawater. *Marine Chemistry*, 8, 347–359. [https://doi.org/10.1016/0304-4203\(80\)90024-9](https://doi.org/10.1016/0304-4203(80)90024-9)
- West, W. E., Creamer, K. P., & Jones, S. E. (2016). Productivity and depth regulate lake contributions to atmospheric methane. *Limnology and Oceanography*, 61, S51–S61. <https://doi.org/10.1002/lno.10247>
- Whitfield, C., Aherne, J., & Baulch, H. (2011). Controls on greenhouse gas concentrations in polymictic headwater lakes in Ireland. *Science of The Total Environment*, 410–411, 217–225. <https://doi.org/10.1016/j.scitotenv.2011.09.045>
- Wiik, E., Haig, H., Hayes, N., Finlay, K., Simpson, G., Vogt, R., & Leavitt, P. (2018). Generalized Additive Models of Climatic and Metabolic Controls of Subannual Variation in pCO<sub>2</sub> in Productive Hardwater Lakes. *Journal of Geophysical Research: Biogeosciences*, 123, 1940–1959. <https://doi.org/10.1029/2018JG004506>

- Wood, S. N. (2017). *Generalized additive models: An introduction with R*, 2nd ed. Chapman and Hall/CRC.
- Wood, Simon N. (2011). Fast stable restricted maximum likelihood and marginal likelihood estimation of semiparametric generalized linear models. *Journal of the Royal Statistical Society: Series B (Statistical Methodology)*, 73(Part 1), 3–36. <https://doi.org/10.1111/j.1467-9868.2010.00749.x>
- Wood, Simon N, Pya, N., & Säfken, B. (2016). Smoothing Parameter and Model Selection for General Smooth Models. *Journal of the American Statistical Association*, 111(516), 1548–1563. <https://doi.org/10.1080/01621459.2016.1180986>
- Yamamoto, S., Alcauskas, J. B., & Crozier, T. E. (1976). Solubility of methane in distilled water and seawater. *Journal of Chemical & Engineering Data*, 21(1), 78–80. <https://doi.org/10.1021/je60068a029>
- Yang, P., He, Q., Huang, J., & Tong, C. (2015). Fluxes of greenhouse gases at two different aquaculture ponds in the coastal zone of southeastern China. *Atmospheric Environment*, 115, 269–277. <https://doi.org/10.1016/j.atmosenv.2015.05.067>
- Yool, A., Martin, A. P., Fernández, C. & Clark, D. R. (2007). The significance of nitrification for oceanic new production. *Nature*, 447, 999–1002. <https://doi.org/10.1038/nature05885>
- Zhang, W., Li, H., Pueppke, S. G., & Pang, J. (2021). Restored riverine wetlands in a headwater stream can simultaneously behave as sinks of  $\text{N}_2\text{O}$  and hotspots of  $\text{CH}_4$  production. *Environmental Pollution*, 284, 117114. <https://doi.org/10.1016/j.envpol.2021.117114>

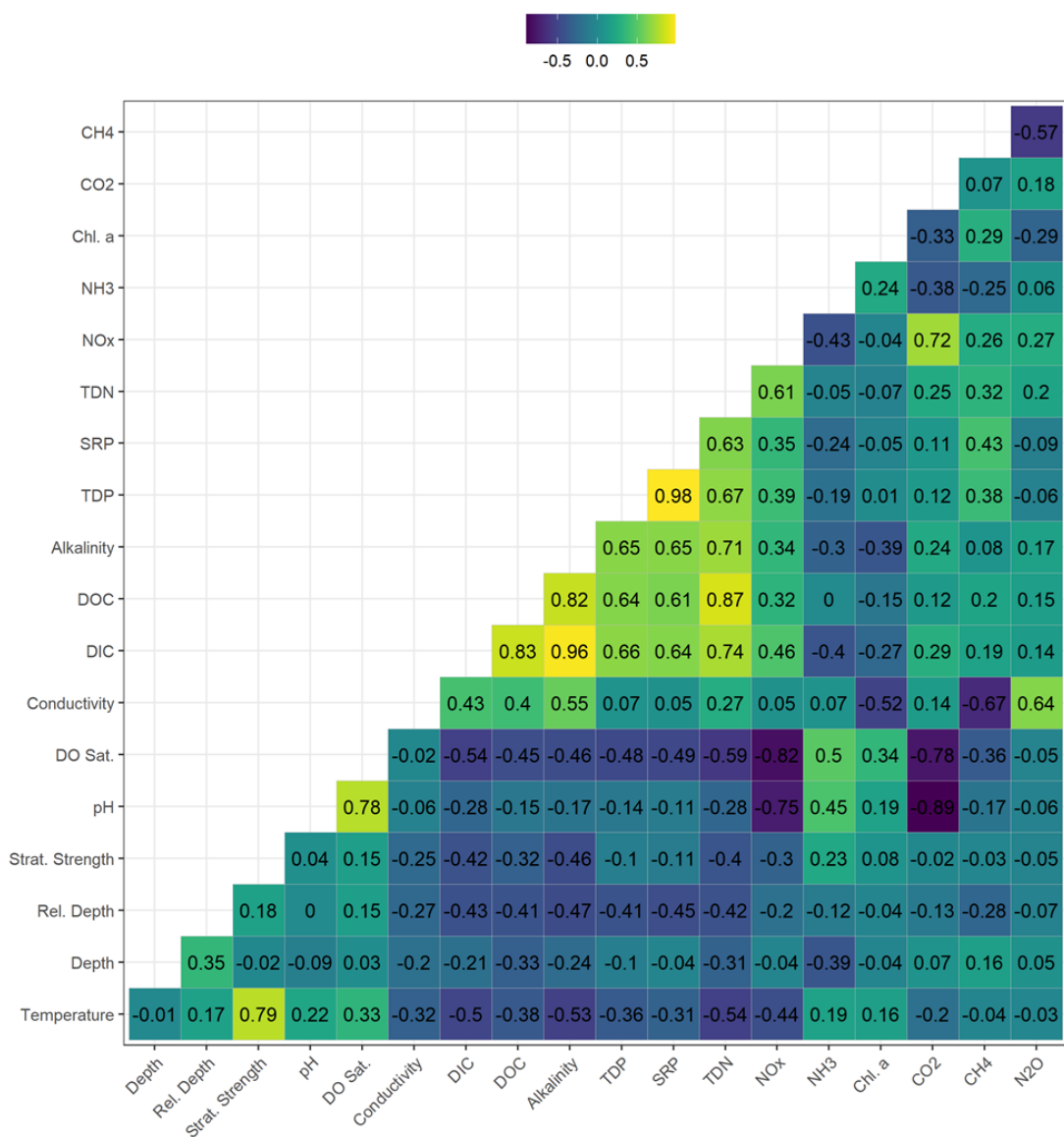


**Figure S1.** Spearman correlation tables showing physical, chemical, and biological variables for agricultural reservoirs. Yellow values indicate high positive correlation, while dark purple values indicate high negative correlation. Rel. Depth = relative depth. Strat. Strength = buoyancy frequency. DO Sat. = surface dissolved oxygen saturation. DIC = dissolved inorganic carbon. DOC = dissolved organic carbon. TDP = total dissolved phosphorus. SRP = soluble reactive phosphorus. TDN = total dissolved nitrogen. NO<sub>x</sub> = nitrate and nitrite. NH<sub>3</sub> = ammonia. Chl. a = chlorophyll a. CO<sub>2</sub> = carbon dioxide. CH<sub>4</sub>



= methane. N<sub>2</sub>O = nitrous oxide.

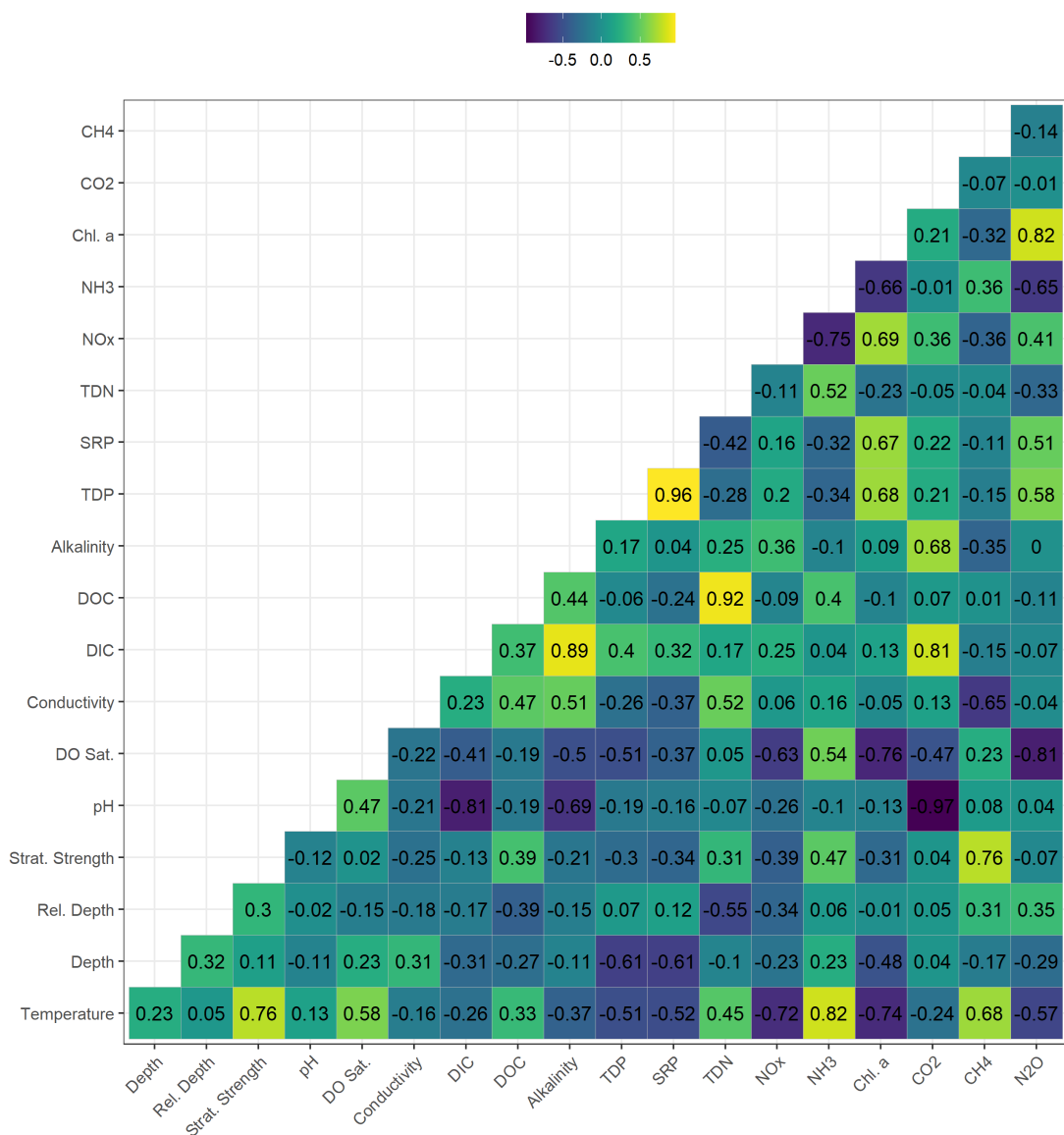


**Figure S2.** Spearman correlation tables showing physical, chemical, and biological variables for natural wetland ponds. Yellow values indicate high positive correlation, while dark purple values indicate high negative correlation. Rel. Depth = relative depth. Strat. Strength = buoyancy frequency. DO Sat. = surface dissolved oxygen saturation. DIC = dissolved inorganic carbon. DOC = dissolved organic carbon. TDP = total dissolved phosphorus. SRP = solu-

ble reactive phosphorus. TDN = total dissolved nitrogen.  $\text{NO}_x$  = nitrate and nitrite.  $\text{NH}_3$  = ammonia. Chl. a = chlorophyll a.  $\text{CO}_2$  = carbon dioxide.  $\text{CH}_4$  = methane.  $\text{N}_2\text{O}$  = nitrous oxide.

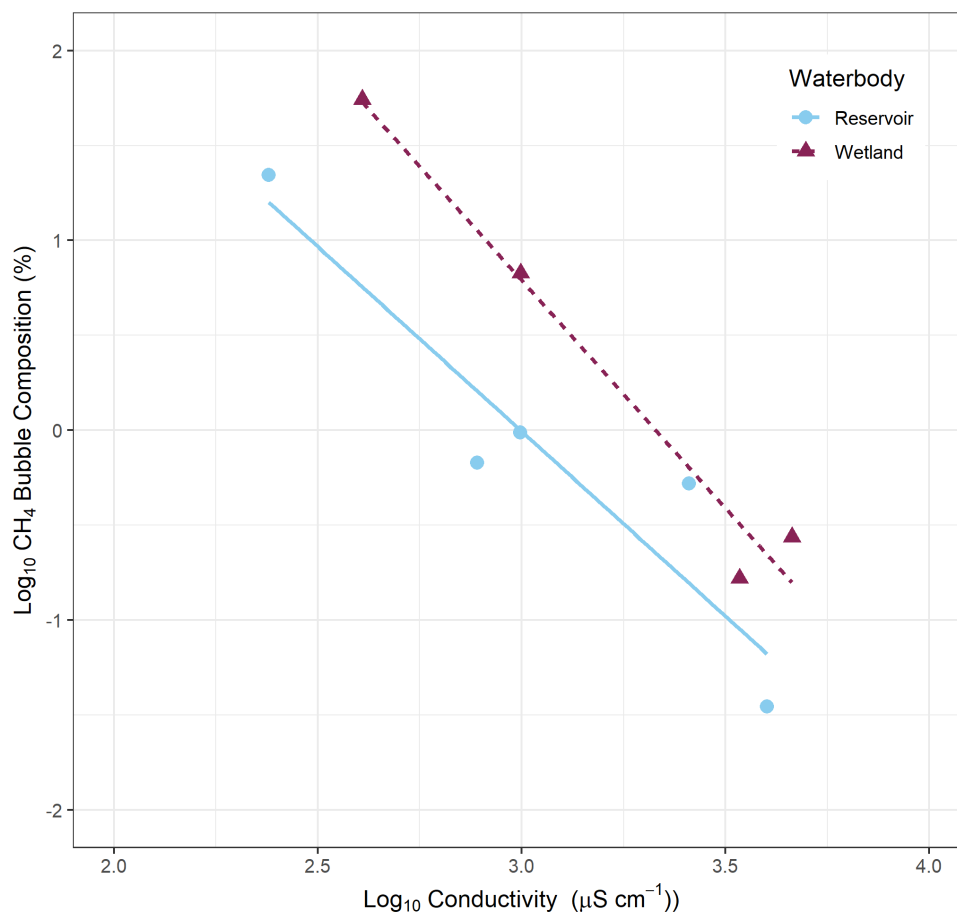


**Figure S3.** Relationship of  $\text{CH}_4$  bubble composition ( $\log_{10}$ ) and conductivity ( $\log_{10}$ ) in agricultural reservoirs (red) and natural wetland ponds (blue). Points indicate the measured values. Lines represent the linear regression line. Reservoir Adj.  $R^2 = 0.8268$  ( $n = 5$ ), wetland Adj.  $R^2 = 0.9504$  ( $n = 4$ ).

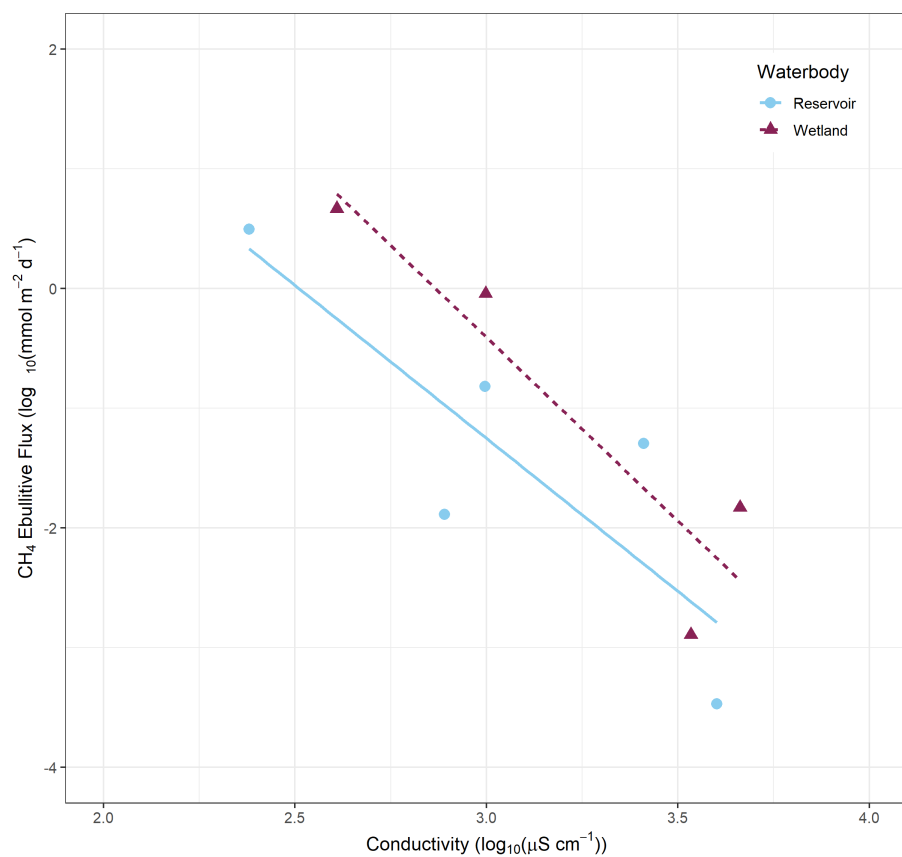


**Figure S4.** Relationship of CH<sub>4</sub> ebullitive flux ( $\log_{10}$ ) and conductivity ( $\log_{10}$ ) in agricultural reservoirs (blue) and natural wetland ponds (red). Points indicate the measured values. Lines represent the linear regression line. Reservoir Adj.  $R^2 = 0.6044$  ( $n = 5$ ), wetland Adj.  $R^2 = 0.7678$  ( $n = 4$ ). CH<sub>4</sub> = methane.